HAL
open science

Hybrid semiconducting nanoplatelets : synthesis and molecule-driven assembly

Yesica Flores

To cite this version:

Yesica Flores. Hybrid semiconducting nanoplatelets : synthesis and molecule-driven assembly. Coordination chemistry. Sorbonne Université, 2018. English. NNT : 2018SORUS464 . tel-02946263

HAL Id: tel-02946263

https://theses.hal.science/tel-02946263v1

Submitted on 23 Sep 2020

HAL is a multi-disciplinary open access archive for the deposit and dissemination of scientific research documents, whether they are published or not. The documents may come from teaching and research institutions in France or abroad, or from public or private research centers.

L'archive ouverte pluridisciplinaire **HAL**, est destinée au dépôt et à la diffusion de documents scientifiques de niveau recherche, publiés ou non, émanant des établissements d'enseignement et de recherche français ou étrangers, des laboratoires publics ou privés.

Sorbonne Université

Ecole doctorale de Chimie Moléculaire de Paris-Centre

Institut Parisien de Chimie Moléculaire / Equipe de Recherche en Matériaux Moléculaires et Spectroscopies

Hybrid semiconducting nanoplatelets: synthesis and molecule-driven assembly

Par Yesica Flores Arias

Thèse de doctorat de Chimie

Dirigée par Benoit Fleury

Présentée et soutenue publiquement le 21 septembre 2018

Devant un jury composé de :

Mme Corinne Chanéac, Professeur	Examinatrice
Mme Nathalie Katsonis, Professeur	Examinatrice
Mr. Vincent Huc, Chargé de recherche	Rapporteur
Mr. Guillaume Rogez, Directeur de recherche	Rapporteur
Mr. Benoit Fleury, Maître de conférences	Directeur de thèse

Dedication

Dedico esta tésis a mis padres, hermanos y a mi segunda alma
por su constante apoyo y profundo amor. Ustedes fueron una roca para mi en los
momentos difíciles. A mis abuelos que no están aquí
pero sé que me miran desde el cielo junto a Dios.
Los amo incondicionalmente.

Acknowledgements

First, I would like to thank all the jury members: Prof. Corinne Chanéac, Prof. Nathalie Katsonis, Dr. Guillaume Rogez and Dr. Vincent Huc for the time taken to evaluate this work. I thank Dr. Guillaume Rogez and Dr. Vincent Huc also for having accepted the role of referee.

I would like to show my appreciation to established scholars of the research group on molecular materials and spectroscopies: Rodrigue Lescouëzec, Laurent Lisnard, Yanling Li and Yves Journaux, Mannan Seuleiman, Alexandrine Flambard and Christophe Cartier-dit-Moulin for the knowledge, helping me, and offering me assistance for my research. I also thank all the present members of the group EPOM.

I also want to acknowledge the generous financial support I received from the ERMMES team during my doctoral studies at the Institut Parisien Chimie Moléculaire and the LabEx MiChem financial support as well as the Réseau Franco-Néerlandais for giving me the opportunity to make two internships at the University of Twente in the Netherland; and of course, the *Consejo Nacional de Ciencia y Tecnología* (Conacyt) for the main financial support I received to make possible a dream, my Ph.D.

I would like to extend my acknowledgements to Corinne Chanéac for giving us access to the infrastructures of LCMCP and for the support and encouragements during my Ph.D. I would like to address special thanks to Nathalie Katsonis for the invaluable learning obtained through the stays in Enschede.

To He, I thank him for welcoming me during my stay in Enschede.

To my former and current colleagues Rémi, Juan, Ammar, Emmanuel, Amina, I thank them for their support, for helping me, and for the good times we spent together on this long journey, I really appreciate it. A big thank to Julian for all and to Qui. To Ang, I thank him for his priceless help, for his kindness, support and for all the fun we have had in the last 3 years. To Maxime and Jana I thank them for sharing an invaluable time, for your help, for all the fun at the lab and for encouraging me during my writing. I am happy to have shared my last year with you. Best wishes to all of them.

I would also like to thank Richard who was instrumental in helping me out with Raman Characterization and to analyze the data. More importantly, for been very supportive, for teaching me, for cheering me up, for having a positive outlook, for been enthusiastic, energetic, for all the pleasant conversations and for making me smile at every moment. You are an incredible person.

A special thank to my Ph.D. advisor Dr. Benoit Fleury for supporting me during these past 3 years, for the countless insightful discussions about research, knowledge, and suggestion in general. Even more, I thank you for your kindness, patience, optimism, for the amusing conversations, for guiding me, for cheering me up, for the opportunity you gave me to do my Ph.D, and to pursue new projects, and most important for driving me to give the best of myself. You have been an excellent mentor, instructor, and teacher. Benoit you are an extraordinary person.

I also thank my friends Eunice, Lupita and Rafa for their support and priceless friendship.

I would like to especially thank my other soul and my wonderful family for the deep love, caring, constant support and encouragement that I have had over my all life. In particular my parents, my beloved sister and brother that have sacrificed a lot for me. I love them so much and I would not have made it this far without them.

Table of contents

Introduction 2
Chapter I: Semiconducting nanocrystals 8
I.1 Definition 8
I. 2 Optical properties of CdSe semiconductor 10
I. 3 Synthesis 12
I. 3. 1 Physical methods 12
I. 3. 2 Chemical methods 12
I. 4 Shape control 15
I. 4. 1 Kinetic control 15
I. 4. 2 Shape control by the surfactants 16
I. 5 CdSe Nanoplatelets: synthetic aspects 17
I. 6 Optical properties of CdSe nanoplatelets 21
I. 6. 1 Effect of the NPLs thickness and lateral dimensions 23
I. 6. 2 Effect of the ligand 24
I. 7 Self-assembly of CdSe nanoplatelets 26
I. 8 References 34
Chapter II: Dynamic assembly of CdSe nanoplatelets into superstructures 38
II. 1 Self-assembly 38
II. 1. 1 Concept 38
II. 1. 2 Types of assembly 39
II. 1. 3 Assembly of nanoparticles 40
II. 1. 4 Motivation of this work 42
II. 2 Azobenzenes 43
II. 3 Synthetic strategy 44
II. 4 First generation of azobenzene ligands: C3, C11 and C18 46
II. 4. 1 CdSe nanoplatelets purification 46
II. 4. 2 Ligand exchange 46
II. 4. 3 Results and discussion 46
II. 5 Second generation of azobenzene ligands: tBuC3, tBuC11, tBuC18 49
II. 5. 1 NPLs treatment 49
II. 5. 2 Ligand exchange 49
II. 5. 3 Results and discussion 49

II. 6 Conclusion and outlooks 54
II. 7 Methods 56
II. 8 References 57
Chapter III: Composite materials made of CdSe nanoplatelets and metallophthalocyanines.. 61
III. 1 Phthalocyanines 62
III. 1. 1 Structures 62
III. 1. 2 Solubility issues 63
III. 1. 3 Electronic properties of cobalt phtalocyanine 63
III. 2 Composite material made of CoPc and CdSe NPLs by addition of a bridging ligand 65
III. 2. 1 Synthetic strategy 65
III. 2. 2 Results 67
III. 2. 3 Discussion 71
III. 3 Composite material made of CoPc and CdSe NPLs by weak interactions 72
III. 3. 1 Synthetic strategy 72
III. 3. 2 Results and discussion 73
III. 4 Conclusion and perspectives 77
III. 5 Experimental section 79
III. 6 References 81
Conclusion 84
Annex A 87
Annex B 88

Introduction

Introduction

Nowadays, significant progresses have been made in developing nanomaterials like nanoparticles due to their promising potential in nanodevices with future applications in the fields of biomedicine, chemistry, electronics, and optics. Over the past decade, excellent methodologies have been developped for controlling their size, morphology and crystalline phase.[1] However, the realization of emerging convergence technology requires to have the capability to observe, understand, control, and even to predict the reactivity of materials at multiscale levels including, nano, micro, and macro scales.

The connection among different scales is necessary for producing novel nano-electric/optical/magnetic devices and nano-energy devices revealing extraordinary and original performances.[2] Such unification among different levels in three-dimensions is referred to as three-dimensional architecture. The creation of such unification is difficult and challenging, but also worthwhile to explore owing everything can entail.[2]

In the last two decades, colloidal semiconductors nanocrystals like quantum dots (QDs) have generated strong interest thanks to their tunable spectroscopic properties due to quantum confinement, making them promising materials for the application in various fields such as lighting technologies and bioimaging.[3] These nanomaterials are made of cadmium chalcogenides, such as CdS, and CdSe since the photoluminescence and absorption band is located in the visible range.[4] However, despite the implicit toxicity concerns,[5] the cadmium selenide (CdSe) QDs are popular because of their facile synthesis and potential ability, although challenging, to develop hybrid, and composite nanomaterials, which is the particular interest in this work. Very recently our group was able to graft coordinating complexes such as Mn(II) complexes at the surface of QDs, revealing promising magneto-optics properties since after illuminating at 532 nm laser light on the hybrid QDs, their magnetization increases suggesting ferromagnetic alignment of Mn(II) ions. Colloidal semiconductor nanocrystals can be synthesized in various shapes and size.[4] In semiconductors, an important criterion is the shape, because it strongly modifies the electronic properties.[6]

In 2008, the synthesis of quantum wells, also known as nanoplatelets (NPLs) by Dubertret and coworkers was reported.[7] These semiconducting colloidal nanoplatelets have a

zinc blende structure. These ultrathin and flat nanocrystalline colloids exhibit outstanding optical properties, which are tunable by controlling their vertical thickness.

From a chemical outlook, these new materials are attractive to study because they have precisely defined facets (that are capped with organic ligands), making them a model system to understand the influence of surface chemistry.[8] These nanoplatelets with their unique physical properties and well-defined chemistry encourage us to give the next step to the development of new hybrid materials. However, to the best of our knowledge, the existence of hybrids NPLs has not been observed or studied yet.

Despite the scarce significant references in the field of hybrid nanoplatelets, we decided to create new hybrids NPLs by the incorporation of inorganic molecules (annexes). Experimentally, this task was difficult since the NPLs stability as well as their optical properties are often ultimately limited by the performance of the ligand that binds the surface of the NPLs, quenching their photoluminescence and in most cases destroying them.

Recently, Abécassis *et al*, have reported that the assembly of NPLs in solution was obtained upon the addition of an antisolvent[9] and upon the incorporation of an excess of oleic acids[10] giving long micrometer needles. Interestingly, the assembly of the nanoplatelets emits polarized light[9] and the interaction between the quantum well within stacks trigger the appearance of a phonon replica at low temperature.[11] Thanks to these favorable features we further developed a new system that reversibly induces the formation of long superstructures made of nanoplatelets.

In chapter 2, the strategy starts with the functionalization of the NPLs with azobenzenes molecules specially designed to anchor the surface of the nanoparticles. These azobenzene ligands synthesized in Enschede by the group of Prof. Nathalie Katsonis are photoswitchable molecules that go through a *trans* to *cis* isomerization upon UV illumination, triggering the NPLs assembly. With the aim to further characterize the assembly properties of these nanoplatelets, I did two internships at the University of Twente in Enschede thanks to the MiChem Labex and French-Dutch network for higher education and research, whom provided me an *Eole* scholarship. The experience left us with a conceptual idea of evolving and improving the system.

The next big step of the work was to evolve from colloidal hybrids to composite materials. Composite materials are the new generation of novel materials thanks to their dimensional and chemical stability.[12] They are made from mixing two or more materials with different physical and chemical properties with the aim to control and develop new and unprecedented structures. The special properties of the composites rely on the individual components, their morphology and the interactions between its phases at the inner interfaces. Moreover, semiconductor-based composite materials are attractive material since both absorption and light emission of semiconductors nanoparticles can be strongly affected in the nanometer size, giving them a new dimension to their study.[10] But what will happen if we incorporate a paramagnetic component to these semiconductors? Can collective properties lead to original magneto-optical behaviors? In chapter 3, in order to answer these questions, we develop semiconductor-based paramagnetic composite materials by the interaction between semiconductor nanoplatelets and paramagnetic molecular complex like the cobalt phthalocyanine (CoPc) molecule.

References

1 L. Wang, Y. Rho, W. Shou, S. Hong, K. Kato, M. Eliceiri, M. Shi, C. P. Grigoropoulos, H. Pan, C. Carraro and D. Qi, Programming Nanoparticles in Multiscale: Optically Modulated Assembly and Phase Switching of Silicon Nanoparticle Array, *ACS Nano*, 2018, **12**, 2231–2241.

2 H. Sung and M. Choi, Assembly of Nanoparticles: Towards Multiscale Three-Dimensional Architecturing, *KONA Powder and Particle Journal*, 2013, **30**, 31–46.

3 K. Das, S. Sanwlani, K. Rawat, C. R. Haughn, M. F. Doty and H. B. Bohidar, Spectroscopic profile of surfactant functionalized CdSe quantum dots and their interaction with globular plasma protein BSA, *Colloids and Surfaces A: Physicochemical and Engineering Aspects*, 2016, **506**, 495–506.

4 A. Antanovich, A. Prudnikau, A. Matsukovich, A. Achtstein and M. Artemyev, Self-Assembly of CdSe Nanoplatelets into Stacks of Controlled Size Induced by Ligand Exchange, *The Journal of Physical Chemistry C*, 2016, **120**, 5764–5775.

5 Y. Zhang, A. M. Schnoes and A. R. Clapp, Dithiocarbamates as Capping Ligands for Water-Soluble Quantum Dots, *ACS Applied Materials & Interfaces*, 2010, **2**, 3384–3395.

6 S. Ithurria, M. D. Tessier, B. Mahler, R. P. S. M. Lobo, B. Dubertret and A. L. Efros, Colloidal nanoplatelets with two-dimensional electronic structure, *Nature Materials*, 2011, **10**, 936.

7 S. Ithurria and B. Dubertret, Quasi 2D Colloidal CdSe Platelets with Thicknesses Controlled at the Atomic Level, *Journal of the American Chemical Society*, 2008, **130**, 16504–16505.

8 E. Lhuillier, S. Pedetti, S. Ithurria, B. Nadal, H. Heuclin and B. Dubertret, Two-Dimensional Colloidal Metal Chalcogenides Semiconductors : Synthesis, Spectroscopy, and Applications, *Accounts of Chemical Research*, 2015, **48**, 22–30.

9 B. Abécassis, M. D. Tessier, P. Davidson and B. Dubertret, Self-Assembly of CdSe Nanoplatelets into Giant Micrometer-Scale Needles Emitting Polarized Light, *Nano Lett.*, 2014, **14**, 710–715.

10 S. Jana, P. Davidson and B. Abécassis, CdSe Nanoplatelets: Living Polymers, *Angewandte Chemie International Edition*, 2016, **55**, 9371–9374.

11 M. D. Tessier, L. Biadala, C. Bouet, S. Ithurria, B. Abecassis and B. Dubertret, Phonon Line Emission Revealed by Self-Assembly of Colloidal Nanoplatelets, *ACS Nano*, 2013, **7**, 3332–3340.

12 R. Sahay, V. J. Reddy and S. Ramakrishna, Synthesis and applications of multifunctional composite nanomaterials, *Int J Mech Mater Eng*, 2014, **9**, 25.

13 K. Rajeshwar, N. R. de Tacconi and C. R. Chenthamarakshan, Semiconductor-Based Composite Materials : Preparation, Properties, and Performance, *Chem. Mater.*, 2001, **13**, 2765–2782.

Chapter I: Semiconducting nanocrystals

Chapter I: Semiconducting nanocrystals

I.1 Definition

Colloidal semiconducting nanocrystals (NCs) are crystalline particles containing some hundreds to a few thousands of atoms. These compounds are based on an inorganic core, enclosed in an organic outer layer of surfactant molecules called ligands.[1]

The physical important parameter of semiconducting materials is the width of the energy gap, which is the minimum energy required to promote an electron from the ground state valence energy band to the conduction energy band (see Fig.1), forming an exciton.[2] The energy gap is a fixed parameter in solids of macroscopic size and depends on the material's nature. The situation is different in nano-semiconductors with sizes smaller than ~ 10 nm, because of their dimensionality and quantization. This gap is related to the quantum system for which electronic excited states feel the presence of the particle border. The electronic levels respond to any change in the particle size by adjusting their energy. This feature is known as quantum confinement, and the nanomaterials with this characteristic are referred to as quantum dots (QDs).[3,4]

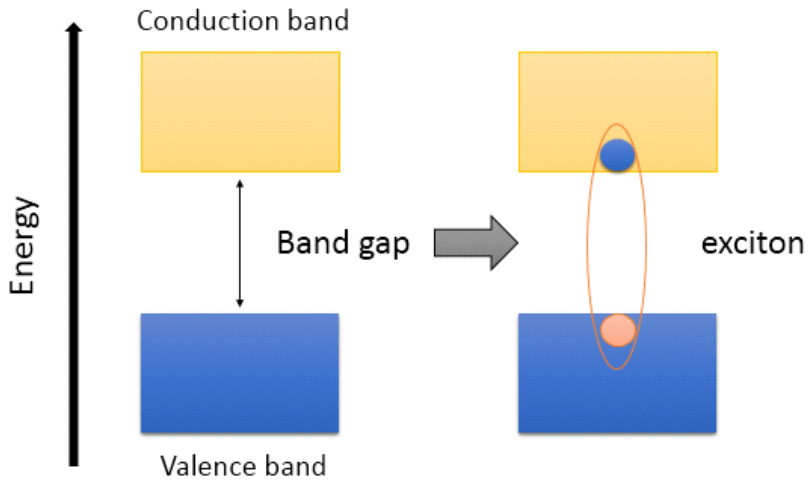

Figure 1. Formation of an exciton

Colloidal quantum dots can be considered as an intermediate class of material between atoms and bulk. The comparison between the energy levels of nanocrystals and bulk semiconductors on the one side and molecular structures on the other side is exemplified by the figure 2.

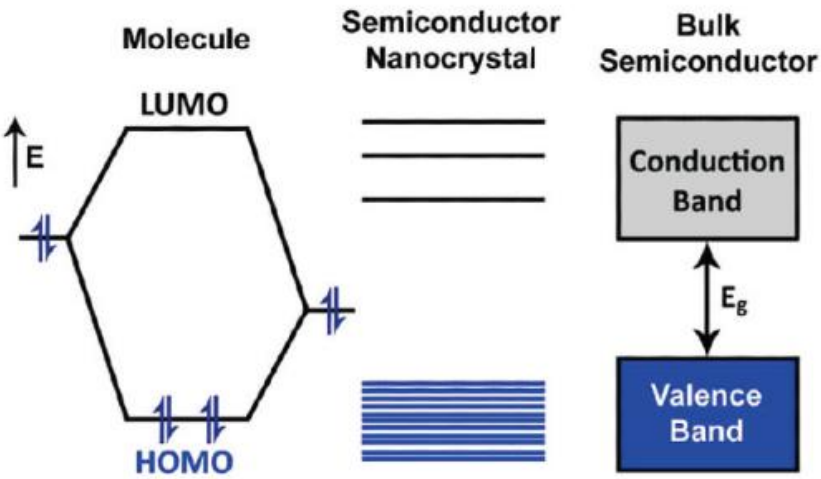

Figure 2. Evolution of electronic levels from molecule to bulk material

Nanocrystals are classified according to the categories given by Pokropivny and Skorokhod (2007)[5] in:

- (3D) Three-dimensional structures (nanocups).
- Two-dimensional (2D) structures such as nanofilms, nanosheets, nanoplatelets (NPLs), etc.
- One-dimensional (1D) materials as nanowires (NWs), nanorods (NRs),
- Zero-dimensional (0D) structures as nanospheres, nanodots, etc.

In bulk semiconductors, the exciton can move freely in all directions. When the size of the nanocrystals semiconductors is smaller than the radius of Bohr of the exciton, the charge carriers (electron and hole) become spatially confined; this effect is known as quantum confinement regime. Therefore, the exciton's size outlines the transition between the bulk crystal properties and the quantum confinement. The quantum confinement displays size-dependent absorption and fluorescence spectra. In addition, depending of the degree of confinement and the dimensionality, the band gap can be tuned to a define energy.

I. 2 Optical properties of CdSe semiconductor

CdSe nanoparticles are II-VI semiconductors with interesting optical properties determined by their size and structure. The conduction band is typically composed of the s orbitals of cadmium, which is degenerate twice by the electron spin. The conduction band commonly consists of the orbitals p_x, p_y, *and* p_z of selenium and is degenerated 6 times by the hole spin and the orbital moment. The valence band also comprises three bands, heavy holes (hh), light holes (lh) and the split off bands (so). The II-VI semiconductors usually present an interaction between the spin *s* and the orbital moment *l* of a particle resulting in a quantum number ($J = s + l$). In the valence band, the quantum number *J* takes different values in the hole bands ($J_h = 3/2$ and $J_h = 1/2$) and they are separated by an energy Δ_{so}. In the case of the würzite structure, the hh and the lh are separated by an energy Δ_{int} (Fig. 3).[6]

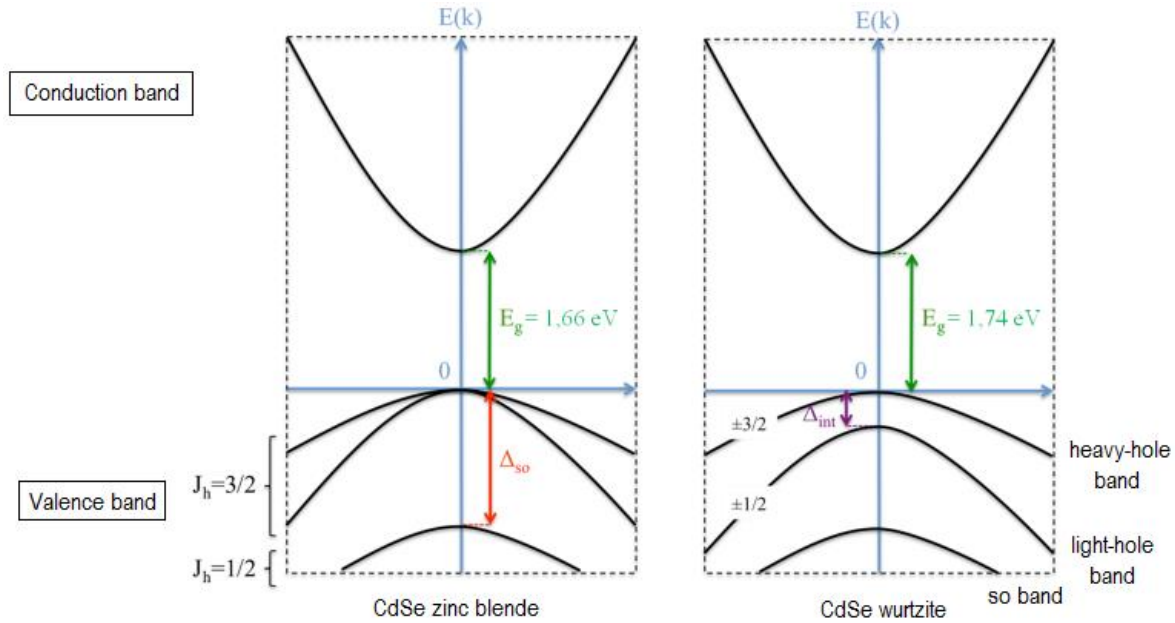

Figure 3. Schematic representation of the energy band structure of zinc blende and würzite CdSe nanocrystals.

The spacing between the bands diminishes when atoms are added to the particle. When the semiconducting nanocrystals are of the same composition but of different sizes their optical properties change. Upon excitation at energy bigger than the band gap an electron-hole pair (exciton) is created between the valence and the conduction band. This is noticeable on the UV-visible absorbance spectra (Fig. 4). For incident energies below the band gap the material does not absorb light. For an incident energy corresponding to this gap,

one can observe a transition known as the excitonic transition. And for even higher energies, the absorbance continuously increases since all transitions in the conduction band can occur. The exciton then relaxes in a radiative manner leading to a photoluminescence (PL) spectrum made of a single narrow peak corresponding to the splitting between the band edges. As consequences, since the bigger the nanocrystals are the smaller the gap is, the emission color of the band-edge PL shifts continuously, towards lower energies, as the size of the nanocrystals increases, and so does the excitonic transition in absorbance (Fig. 4). The distance between the electron and hole in a semiconductor is known as the Bohr radius of the exciton (a_B). The minimum value for the band gaps corresponds to the bulk material, value that can be reached when the radius of the crystals is of the order of the Bohr radius of the exciton.[1]

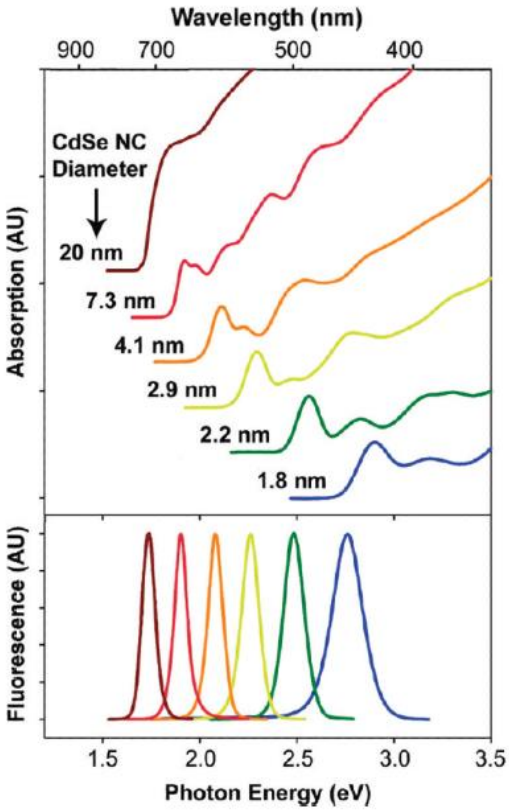

Figure 4. UV- visible spectra of various size QDs (top). Size-tunable fluorescence of quantum dots (bottom).

I. 3 Synthesis

Over the past several years considerable effort has been placed on the controlled synthesis of semiconducting nanocrystallites. Achieving an appropriate high quality synthetic method is crucial to interpreting optical properties, and such an interpretation can be challenging because of different phenomena associated to polydispersities in size and shape and poor crystallinity.[7] QDs have been prepared by physical and chemical methods:

I. 3. 1 Physical methods

Thermal evaporation (TED) is a physical vapor deposition (PVD) technique usually applied to fabricate an extensive range of thin films. This technique is performed in vacuum and the solid precursor is heated at high temperature (above its melting point) until its evaporation. The stream of vapors moves towards a substrate and condenses in the form of thin films. This method allows a better control of different parameters such as thickness, composition, grain size, morphology. For instance, CdS and ZnS of one-dimensional nanoshape such as nanowires and nanoribbons were fabricated on silicon substrates in the presence of Au catalyst by thermal evaporation. The temperature and the concentration of the subtrates were the critical experimental parameter for the formation of different morphologies.[8,9]

Electron beam evaporation is assigned as electron beam physical vapor deposition. In this method, an energetic beam of electrons strikes the material source in a vacuum container and the atoms at the surface collect enough energy to evaporate. The evaporated atoms condense in the form of a coating on the substrate. Electron beam evaporation produces attractive control deposition and morphology with low contamination.[5]

These vacuum techniques have not been studied during this Ph.D. since we intended to develop a soft method to synthesize colloidal hybrid nanocrystals.

I. 3. 2 Chemical methods

The physical methods described above present two main disadvantages: *i*) they require ultra-high vacuum technologies that are expensive and heavy to process and *ii*) QDs are produced in small quantities. Therefore chemists have sought to produce inexpensive and bench experiments able to easily produce batches of colloidal nanocrystals. Here we will

shortly present an overview of different synthetic techniques to produce colloidal nanocrystals.

The solvothermal process[5] involves the chemical reaction of precursors using organic solvents, performed at a temperature that is higher than the boiling point of the solvent. In this method, physicochemical reactions take place at high pressure and temperature. This is so because the growth process is carried out in a container known as autoclave (made of Teflon/stainless steel). Precursors and solvents react at a specific temperature for different durations. The process introduces organic solvents such as long alkylamines (octadecylamine) and more recently short-chain alkylamines (ethylenediamine). The structure, morphology, size, crystal shape and properties of the semiconductor nanocrystallites are strongly influenced by different parameters such as solvent, temperature conditions, precursors, concentration and processing time. The solvothermal technique uses a simple and nontoxic solution route, without tedious size-selection processes and expensive organometallic/non metallic precursors. The advantages of this environment-friendly solvothermal technique include the production of size controlled monodisperse nanocrystals like nanospheres, nanowires, nanorods and nanotripods.[5,10] For instance, nanorods of CdE (E=S, Se, Te) have been successfully synthesized with a solvothermal method.[11]

The Sol-gel method[5] is a chemical synthesis route used to make materials via polycondensation of molecular species from a solution. This method usually consists of dispersed colloidal particles in a solvent (a sol), which is chemically converted into a gel (aggregated sol particles) followed by condensation in the form of solid nanostructures. Sol-gel is a wet chemical method that embraces 2 steps: the first comprises hydrolysis and polycondensation reactions of the precursors to prepare the gels, and the second is sintering of amorphous colloidal into compact powder. This process facilitates the production of nanospheres and nanorods.

Pyrolysis (or hot injection) is one of the most used techniques for the production of high quality nearly monodisperse samples of CdS (E= S, Se, Te) nanometer size crystallites. The synthesis begins with the rapid injection of metal-organic precursors into a hot coordinating solvent (120-360°C) to produce temporally discrete homogenous nucleation. CdSe QDs can be prepared from a variety of cadmium precursors, as alkyl cadmium compounds and some cadmium salts (cadmium oxide, cadmium acetate and cadmium carbonate) combined with a selenium precursor at room temperature (r.t), which is prepared

by dissolving Se powder in trioctylphosphine (TOP) and making a TOP-Se complex. The reagent mixture is rapidly injected to the hot surfactant solvent TOPO (180-210°C°) that results in a short burst of homogeneous nucleation, which is quickly quenched by the fast cooling of the introduction of room temperature reagents.[37] One of the main disadvantages of the pyrolysis process was that it required special experimental precautions because of the extreme high reactivity of the cadmium precursors that also used to restrain the size of the batches.[1] Nevertheless, this problem has been solved over the past decade by using cadmium oxide as stable precursor.

The template method is an easy technique commonly used to prepare nanomaterials.[12] Compared to traditional techniques, the template route allows the efficient control of particles' size, structure and morphology. This technique includes three steps. The first is the preparation of the template. Second, another synthetic approach as sol-gel and hydrothermal method is employed to prepare the main material based on the function of template. Third, the template is removed. The template method is usually divided in 2 groups depending on the use of a hard template or a soft template.

The hard template is a rigid material that controls the dimensions and the morphology of the material.[12] For the preparation of nanomaterials, using porous materials, the precursor is likely to crystallize outside or inside of the pores of the template. The dimension of the pores will contain the unit cell of the material and will form a crystal material, having the same structure as the pore. The material obtained by this process presents good dispersity and homogenous size. However, the removing of the templates usually causes the collapse of part of the pores structure, which affects the final product.

The soft template method requires simple equipment and usually allows good reproducibility.[12] It begins with the formation of an aggregate of organic molecules (surfactants, polymers) by intermolecular interactions. And these aggregates are used as templates. On the surface of or inside these templates some inorganic species are deposited by different methods to form particles with different sizes and shapes. Surfactants and polymers are often used as templates. One of the disadvantages of the method is the stability of the aggregates: ordered structures are formed only if the template has a strong interaction with the precursor.

I. 4 Shape control

The study of the formation and shape evolution of colloidal semiconducting nanocrystals are of great importance to understand the nucleation and growth process. The nucleation is the first step in the growth of any nanocrystal. Through a fluctuation of the medium in which the nanocrystals are formed, several atoms assemble to a small crystal seed that is thermodynamically stable, and thus does not fall into free atoms or ions.[1] Then, growth can be controlled by the kinetics of the reaction or the use of surfactants.

I. 4. 1 Kinetic control

The control of the growth kinetics of II-VI semiconductors can modify the shape of the particles from a spherical to rod morphology. This also implies that kinetic control can be used to manipulate the average particle size and size distribution. The model of LaMer and Dinegar[3] exemplifies the correlation between the solute concentration and different reaction periods. The model includes three periods that start by a supersaturation (I), then a nucleation event (II) followed by a rapid growth (III) and finally by a slower growth by Ostwald ripening (IV) (Fig. 5). Peng *et al*. further studied the growth of CdSe nanocrystals and observed the shape evolution from dots to rods. They showed that the growth process also develops in two steps, related to the concentration of the monomers: focusing and defocusing.[13]

The authors reported that chemical potential of elongated nanocrystals is commonly high compared to dot-shaped nanocrystals. This means that the growth of elongated nanocrystals will take place when the chemical potential of the monomers in solution is relatively high, and usually this occurs when the activity of the monomers (monomers concentration) is also high. This means that by simply increasing the monomers concentration in the solution, dot-shaped CdSe nanocrystal were transformed in rod-shaped. When the Cd concentration of the monomer is higher than the solubilities of all the particles, the nanocrystals grow only along a unique axis. And also some variables as ratio and volume of the crystal increase faster which results in a one-dimensional growth stage (1D-growth stage) and the size distribution narrows down. This is the focusing of size distribution, which leads to a close formation of monodisperse colloidal nanocrystals.

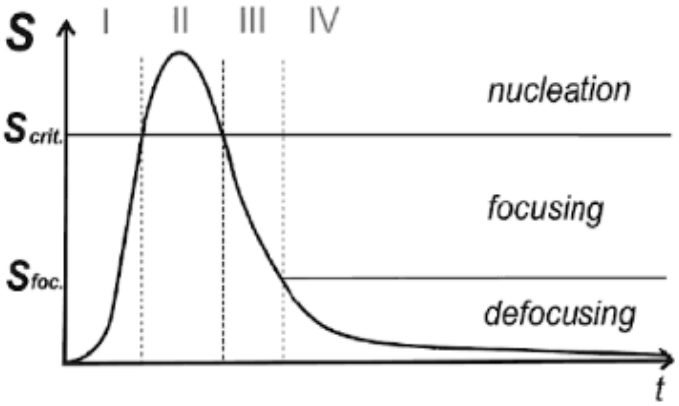

Figure 5. La Mer's model describing the nucleation and growth process for monodisperse colloidal particles.

But if the Cd monomer concentration is at an intermediate level the crystal grows simultaneously in three dimensions. The ratio stays constant and the crystal volume increases. In addition to the concentration of the monomers, thermodynamic parameters (in addition to temperature) also promote the three-dimensional growth. Indeed, when the monomer concentration drops below the critical point, the length of the rods diminished and their width increased and the size distribution broadens. This means that the anisotropic structure is not thermodynamically favourable as the monomers move away from the rod and grow onto the sides promoting one-dimension to two-dimension intraparticle ripening (1D to 2D ripening). In this process with sufficient time, the quantum rods can progress into dot-shaped. This is the defocusing of size distribution (Ostwald ripening).[14,15]

I. 4. 2 Shape control by the surfactants

The performance of surfactants (or surface ligands) has initially been optimized to promote colloidal stability rather than shape and size control. However, surfactants, more than making the nanocrystals dispersible in organic solvents also show extraordinary control over crystal growth at the nanoscale and produce well-defined morphologies.

On the basis of the above facts, to preserve the control of the growth rates, different surfactants need to be used. Peng's group[15,16] further discovered that pure TOPO is not convenient to obtain quantum rods. The presence of pure TOPO induces a faster growth at the high monomer concentration that causes big rod-like particles. The additional components in technical grade TOPO generate slow growth kinetics. To simulate the presence of impurities in technical TOPO (alkyl phosphonic and phosphinic acids - that bind relatively strongly to

cadmium), they add a hexyl-phosphonic acids (HPA) that coordinates stronger than TOPO to cadmium. That allows adjusting the growth rate and improves the shape control of the nanocrystals.

Highly hydrophobic surfactants (e.g double tail surfactants) have been demonstrated to be exceptional shape directing agents over crystal growth at nanoscale due to a better surface passivation ability. Double tail surfactants are more hydrophobic and surface active in comparison to the single tail surfactants. When a surfactant is highly hydrophobic as in the case of didodecyl dimethylammonium bromide (DTAB) the formation of cubes with {100} crystal planes is generated. However weaker hydrophobicity (as dimethylene bis-(dodecyldimethylammoniun bromide) preserves hexagons bound with {111} crystal planes.[17]

The parameters cited above allowed different authors to synthesize CdSe QDs,[18] Q-rods,[19] tetrapods,[20] nanoplatelets[21] and quantum rings (Fig. 6).[22] Among CdSe nanocrystals, we will focus now on nanoplatelets.

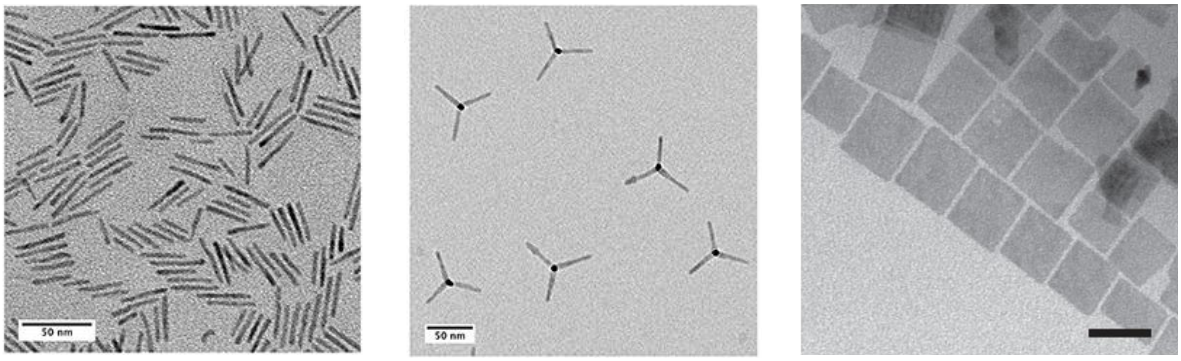

Figure 6. TEM micrographs of different CdSe nanocrystals: from left to right, rods, tetrapods and nanoplatelets.

I. 5 CdSe Nanoplatelets: synthetic aspects

Two-dimensional CdSe semiconductor nanoplatelets or quantum disks have been obtained in two different crystal structures würtzite and zinc blende. The latter has been synthesized by Ithurria and Dubertret in 2008[21] and is one of the most of interesting kind of nanocrystals thanks to their unique optical properties.

An approach to the synthesis of zinc blende nanoplatelets is in some way the soft template method previously mentioned. The synthesis for the CdSe NPLs relies on fatty acid

ligands that bond on the basal planes of the nanoplatelets or quantum disk. To explain, the formation CdSe nanoplatelets, the groups of Peng on the one side and Dubertret, on the other side do not agree on the mechanism of formation of the NPLs and therefore on the best conditions to get them. Dubertret's group, the initiator of nanoplatelets, established that using cadmium acetate ($CdOAc_2$) or short carboxylates as precursor is necessary to trigger the lateral extension of the NPLs. On the contrary, Li and Peng[23] claimed that any fatty acid can be used to get NPLs such as cadmium butanoate ($CdBu_2$), and cadmium octanoate ($CdOc_2$). Nevertheless, both groups concluded that fatty acids are anyway necessary in the synthesis of 2D CdSe nanostructures, either by using these fatty acids as precursors or by adding it during the reaction. In fact, the temperature range of the synthesis is determined by the hydrocarbon chain length of the fatty acids which must be between 140 and 250°C in order to get platelets (Fig.7).

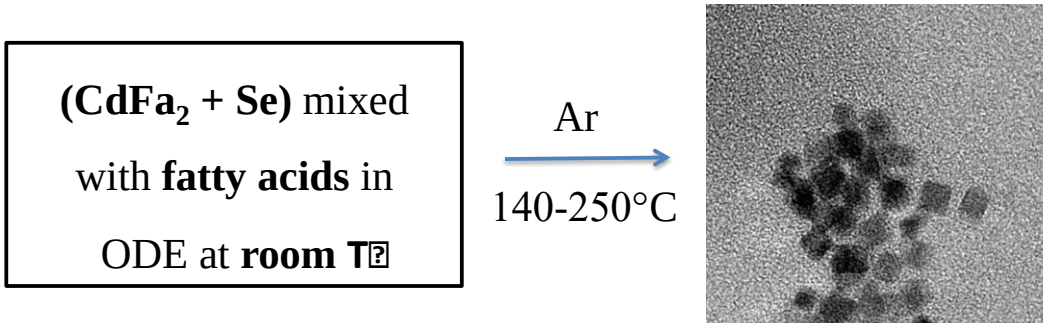

Figure 7. Reaction strategy for obtaining CdSe nanoplatelets. $CdFa_2$ represents the cadmium fatty acid salts.

Among fatty acids that can be used for the synthesis of NPLs, Peng and co-workers tried two fatty acids, stearic acid and decanoic acid (Fig. 8). The results revealed that the up temperature limit increased as the chain length of the fatty acids raised. Therefore, the temperature of apparition of quantum dots occurred early for the dodecanoic acid. The figure 8 show the maximum absorbance of the CdSe nanoplatelets obtained at 180°C for the dodecanoic acid and 240°C for the stearic acid. Li and Peng attributed this effect to the influence of the hydrocarbon chain on the thermal stability of the NPLs, one of the key parameters on the soft-template growth mechanism.

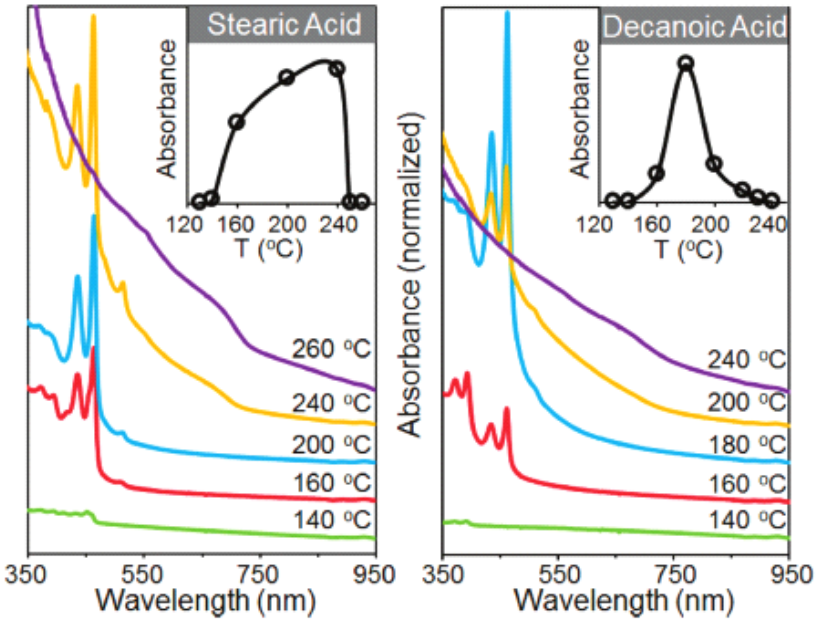

Figure 8. UV-vis of CdSe quantum disks grown at different temperatures and obtained with stearic acid (left) and decanoic acid (rigth). The inset shows the absorbance of the excitonic absorption versus the temperature of the reaction.

It should be pointed out that the lateral dimensions rely upon the concentration of fatty acids, the chain length of fatty acids, and the reaction temperature and the lateral size can be tuned from some nanometers to a few hundred nanometers. It was found that the lower the concentration of the fatty acids the larger the lateral dimension was obtaining. But also increasing the length of fatty acids can lead to the same result. Regarding the effect of the temperature, low temperature resulted in quantum disk of small lateral dimensions.[23] The continuous injection of precursors also induces the growth of lateral extension in different nanoparticles such as CdTe and CdSe NPLs. Another variable to control on these NCs is the thickness.

Further studies[21] demonstrated that the latter the acetates are added to the synthesis the thicker the NPLs would be formed. In the case of CdS, it was shown that low temperature and shorter alipathic chains induce thinner nanoplatelets. The NPLs formation appears between 130 and 140°C in a period of few minutes, the low temperature limit is possibly determined by the activation of elemental Se in the reaction system. The growth of these ultrathin nanocrystals is achieved at higher temperature ranging from 130°C to 250°C whereas at lower temperature the formation of würzite NPLs take place.[24] Higher temperature could eliminate the packing of ligands that is critical for the formation of soft-template process.

Li and Peng also studied the monomers concentration effect on the formation of nanoplatelets. We mentioned in paragraph I.4.1 that in order to get II-IV quantum rods, the concentration of the monomers should be sufficiently high to induce the 1D- growth. However, they didn't found a relevant difference by varying the precursor concentration. One possible explanation is that the Se powder used for the synthesis was no activated, owed to the low temperature reaction used for analyzing.

They also observed that the Cd and Se precursors ratio should be necessary higher than 1:1 for the growth of CdSe disks. This result is consistent with to the fact that in two-dimensional nanocrystals both the top and the bottom are Cd atoms terminated.[23]

Dubertret's group[24] demonstrated that CdSe nanoplatelets growth begins with the nucleation of~ 2 nm diameter nanocrystals seeds. These small nanocrystals would then immediately associate, to form NPLs that gradually expand their lateral dimension (Fig. 9). The formation of nanoplatelets could start by the self-assembly of this well-defined seed to extend laterally (path 1). The self-organization of small cluster that assemble in patches has been observed in ultrathin PbS nanoplatelets with a rock salt crystal structure (path 3). These seeds have two cation-rich facets that are bound to ligands and also can extend laterally thanks to in situ continuous reaction of Cd and Se precursors on the NPLs edges (path 2).

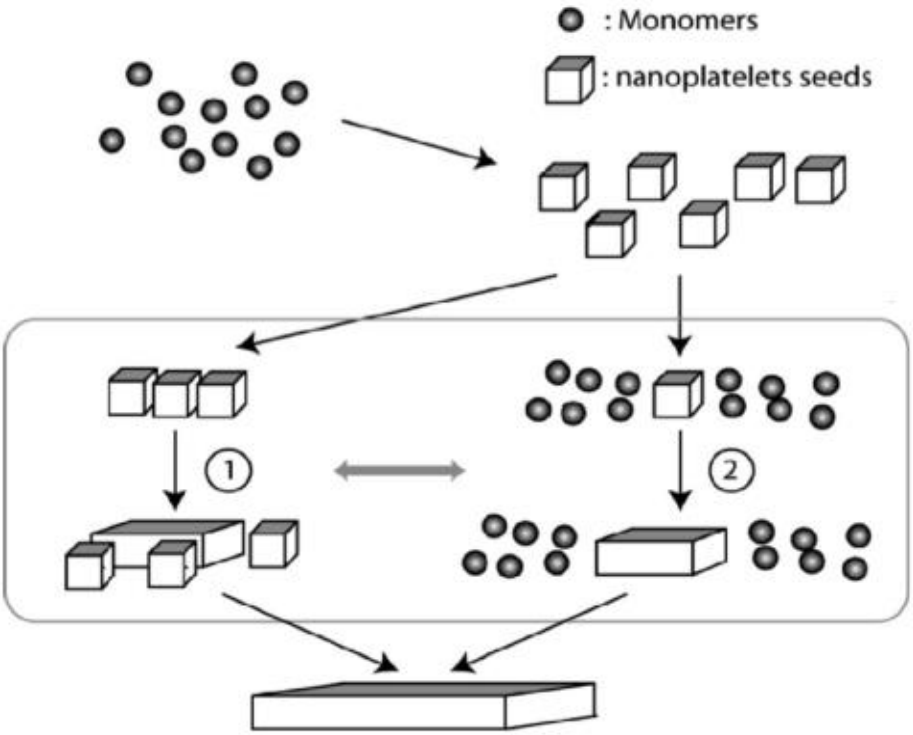

Figure 9. Evolution of the CdSe NPLs lateral extension. It begins with the formation of small seeds. The seeds self-organize to assemble and form the lateral extension (path 1). Lateral dimensions extend by continuous reaction of precursors (path 2).

I. 6 Optical properties of CdSe nanoplatelets

In recent years, colloidal quasi-two dimensional (2D) II-VI semiconductor nanocrystals (NPLs) such as CdS, CdTe and CdSe has gained growing interest due their original optical properties that empower advanced optoelectronic devices. These flat nanocrystals have electronic lateral dimensions that are much larger than the exciton Bohr radius. But their thickness is similar to those of the ultrathin semiconducting quantum wells (QWs).[25]

Cadmium-based nanoparticles offer[26] advantageous features such as a strong oscillator strength and direct bandgaps in the visible region. Thanks to these, many properties of these NPLs such as size, shape, composition, crystal structure or surface ligands can be analyzed by using spectroscopic studies as fluorescence, absorption, photoluminescence excitation and fluorescence lifetime.

Contrary to the würtzite structure the zinc blende NPLs present their thickness along the short axis direction (001). The others two long axis directions correspond to their lateral NPLs planes. The thickness control is quantized to an integer number of monolayers (MLs). Recently, it has been synthesized 3 different populations of nanoplatelets with thickness of 0.9, 1.2 and 1.5 nn. This thickness is characterized by monolayers of CdSe with corresponding numbers of Se layers, which we term 3ML, 4ML, 5ML; maxima of exciton absorption can be found at 463, 513, and 550 nm with lateral dimensions of 60±5 nm by 40±7 nm for 3ML, 27±3 nm by 7±2 nm for 4 ML, 25±3 nm by 10±1 nm for 5ML.[27,28]

The emission quantum yield (QY) has been reported around 50% for the 5ML, between 55 and 34 % for 4ML an 10% for 3ML. The PL lifetime is much faster in NPLs than in 0D QDs, it can go from few nanoseconds at room temperature to 300 ps at 4 K, which makes the NPls the fastest colloidal emitters until now.[29]

For each population of NPLs we can identify on the absorbance spectrum two transitions: a sharp peak that corresponds to the first excitonic transition electron/heavy hole (lowest energy), and a broader signal corresponding to the electron/light hole transition (highest energy). These two transitions are at 513 nm and 480 nm for the 4 ML (Fig. 10).[25]

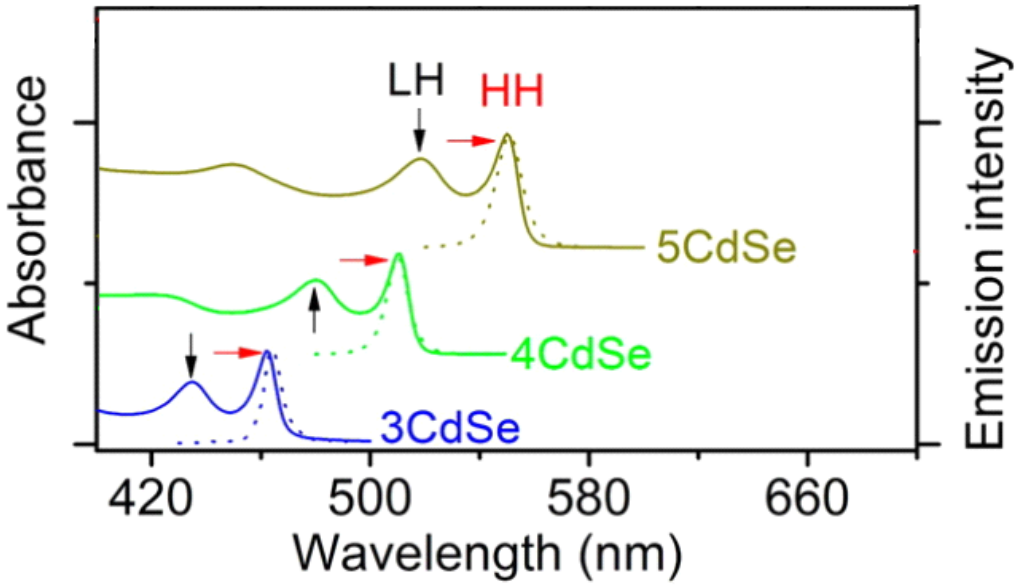

Figure 10. Absorption (solid lines) and photoluminescence spectra (dotted lines) emitting at 462nm (3ML), 512nm (4ML), 550 nm (5ML) CdSe nanoplatelets.

I. 6. 1 Effect of the NPLs thickness and lateral dimensions

The strong quantum confinement in the NPLs is only in the vertical direction, meaning that the only parameter that defines the exciton energy is the thickness of the nanoplatelets.[25] The strong quantum confinement, at the same time, is reflected in a extremely narrow intense bands on both absorption and PL spectra with full width at half maximum (fwhm) close to *kT* tipically between 7 and 10 nm at room temperature and a small Stokes shift.[30,31]

On the other hand, it was reported that increasing the lateral size of NPLS does not produce any spectral shift on PL. However, growing the lateral dimensions has been shown to decrease the Photoluminescence efficiency (PL-QE) and to greatly accelerate the photoluminescence decay rate (Fig. 11). To explain this observation it was found that a broad part of the population of NPLs present hole traps and the probability to find these defects such as Cd vacancy in the CdSe NPLs increases as the lateral area increases. Therefore, this suggests that in ensemble NPLs where the mean lateral size is larger the nonradiative trap channel is introduced by the defected NPls subpopulation.[25]

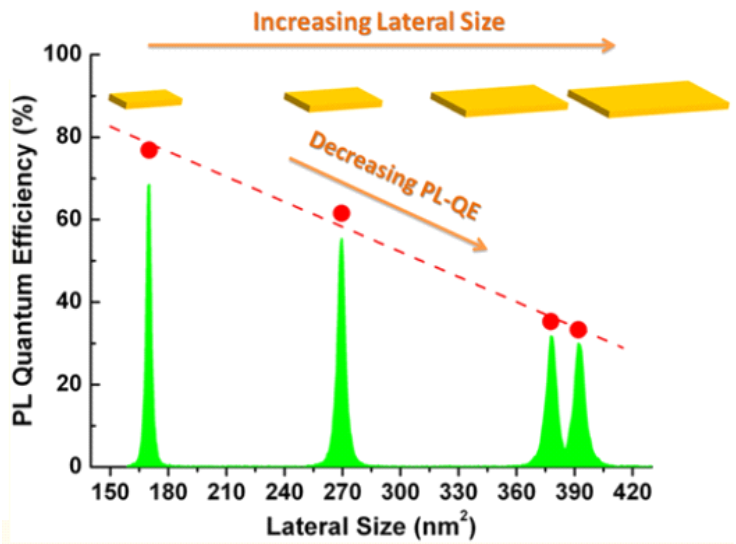

Figure 11. Evolution of the photoluminescence quantum efficiency with increasing lateral size.

Dubretret and co-workers concluded that the zinc blende NPLs presents an atomically flat surface.[26] And being atomically flat enhances the interaction between ligands decorating their surface compared with highly curved surfaces.[31]

I. 6. 2 Effect of the ligand

Ligands play an important role in the colloidal nanocrystal semiconductors properties. For exemple, ligands molecules can be employed as precursors in the synthesis of NCs; they can influence the nucleation and growth kinetic as well as the morphology, size control and crystalline structure of the NCs as we have studied before. They also contribute to the colloidal, chemical and photo-stability in several media by modifying the functionality and reactivity of the NCs. Moreover, it determines significantly the physical properties of the NCs. Among these features, studying the interactions between the ligand and the interphase in the 2D semiconductors nanoplatelets is becoming of great interest.

A key advantage of the NPLs compared to the QDs and nanorods is the surface chemistry, while for QDs and nanorods their highly curved surface introduce disorder in the ligand layer, NPLs present a relatively large and atomically flat surface.

Recently the group of Antanovich[32], evidenced the impact of surface passivating ligands on the optical and structural properties of zinc blende CdSe nanoplatelets. They observed that upon ligand-exchange of native oleic acid (OA) with hexadecanethiol (HDT) and n-hexadecylphosphonic acid (HDPA) on the surface with different monolayers CdSe nanoplatelets the optical spectra become significantly red-shifted (Fig. 12).

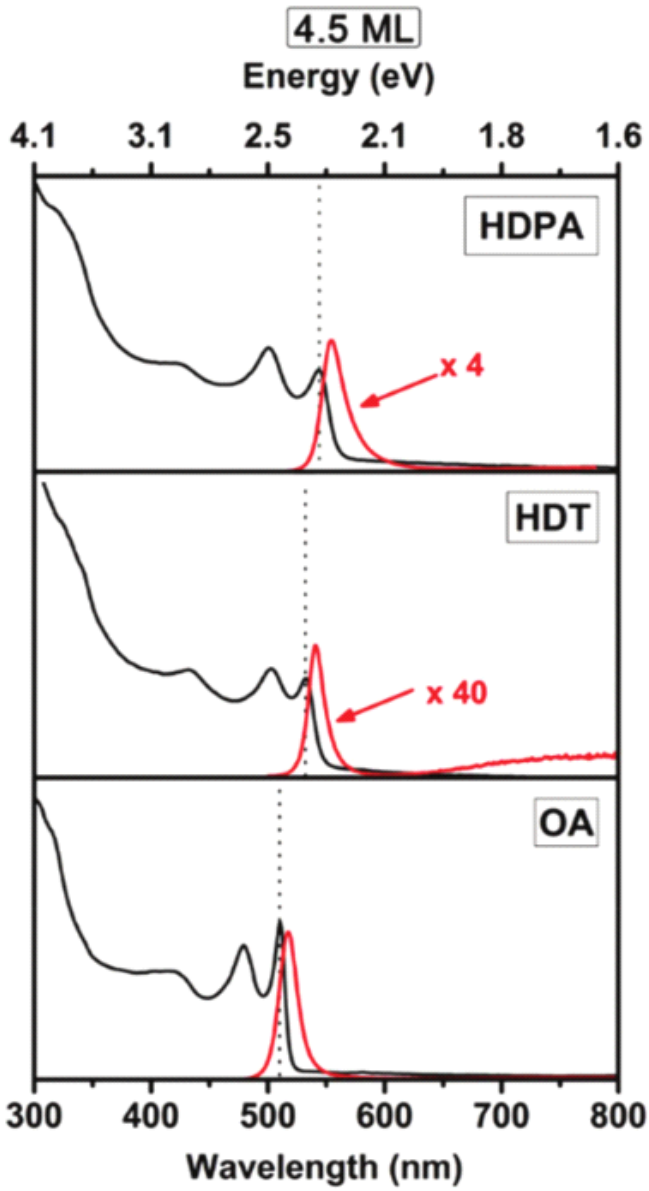

Figure 12. Absorbance (black) and emission spectra (red) of 4ML CdSe NPLs coated with oleic acid (OA), hexadecanethiol (HDT), hexadecylphosphonic acid (HDPA). Dashed lines show the first absorption maxima.

It has been reported for QDs that some capping ligands as phenylchalcogenols Ph-X (X= SH, SeH, TeH) and non-innocent ligands (e.g. phenyldithiocarbamate) can induce large red-shift in PL around 10 -40 nm. Nevertheless, HDPA and HDT are ligands that modify the confinement and exciton transition energy by altering the NCs band gap. They demonstrated that the exciton energy shift was related to structural changes. They exhibited by XRD that the functionalization of the NPLs with organic ligands induces an anisotropic distortion of the unit cell by ligands comprising a contraction of the lateral direction and an expansion in the thickness direction of the ZB unit cell (Fig. 13). This means that cubic symmetry of the ZB

CdSe lattice is diminished into a tetragonal symmetry. Since the lattice distortion can be attributed to several elements, the observed lattice strain magnitude was attributed to the head group interaction with the surface Cd atoms of the NPLs. This assumption is in line with several reports that indicate that an increase of ligand coverage could generate the augmentation of repulsive interaction of headgroups, leading to tensile strain. Therefore, ligand induced strain alters the well thickness and hence the exciton confinement.[32]

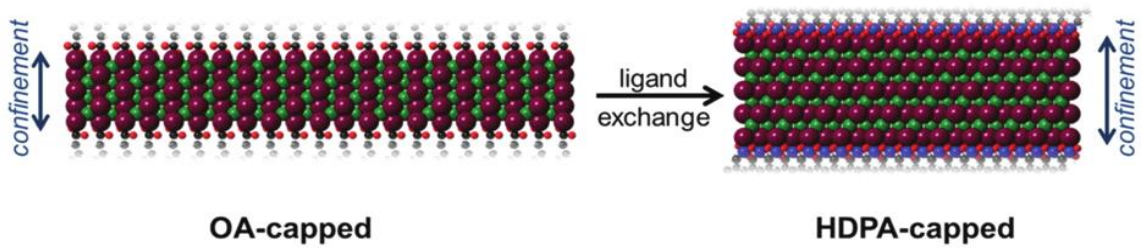

Figure 13. Proposed scheme of anisotropic lattice distortion by ligand exchange.

I. 7 Self-assembly of CdSe nanoplatelets

In 2013, Dubertret and coworkers[33] reported the self-organization of CdSe nanoplatelets into stacks to form 1D-superlattice through the addition of an antisolvent in the colloidal nanoplatelets solution. They noted that addition of ethanol could trigger the formation of anisotropic supracrystals. Hassinen and coworkers[34] exposed that short-chain alcohols remove and replace the carboxylate ligands at the surface of QDs nanocrystals. Therefore, the addition of ethanol could restrain the steric repulsion imposed by the oleic acid brush making possible the nanoparticles stacking. Another explanation comes from the fact that ethanol is a bad solvent for the aliphatic chain of the carboxylate ligands. In other terms, the contact between aliphatic chains of the oleic acids is energetically favoured when the amount of ethanol is increased. In these supraparticles, the NPL building blocks are oriented with their lateral planes that are perpendicular to the long axis of the column-like assemblies, whose length can contain about 10^6 individual nanoparticles (Fig. 14).

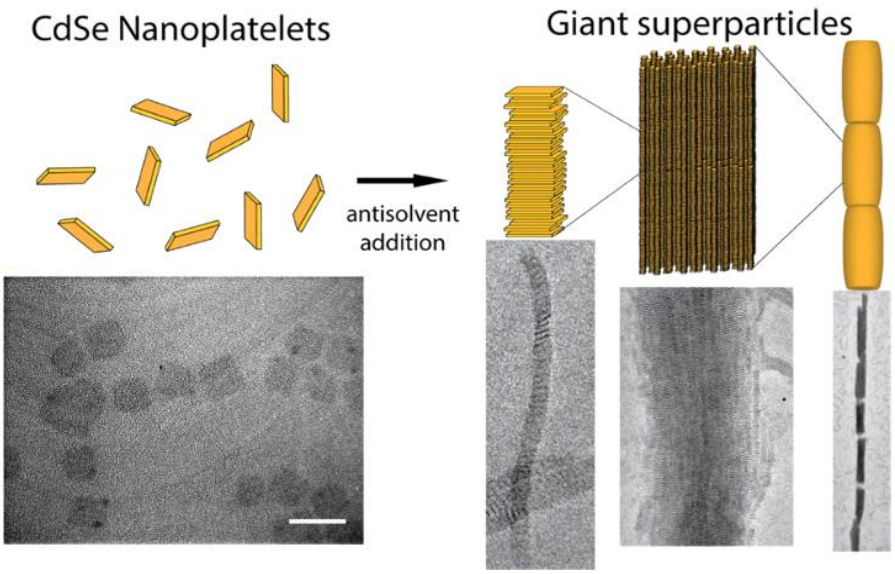

Figure 14. Self-organization of ZB CdSe nanocrystals into 1D superparticles

Interestingly, the light emitted by these microneedles is steadily polarized in the direction perpendicular of the principal direction of the microneedles. This indicate the polarization in the plane of an individual nanoplatelet (Fig 15).[33]

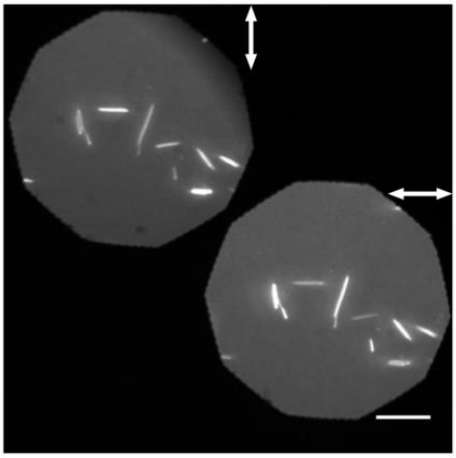

Figure 15. Epifluorescence measurements of stacked NPLs versus the polarization direction.

Another approach to promoting the self-organization of CdSe NPLs is by the slow evaporation of colloidal solution. Abécassis and coworkers used oleic acid followed by a slow drying and then a redispersion to induce the self-assembly into micrometre-long threads. They detected by fluorescence microscopy that these threads can periodically break and restore dynamically. Moreover, free NPL join to both terminations of the existing threads with no formation of new chains. In other terms, the length of threads increases through the addition

of NPLs (Fig. 16). For this reason the 1-dimensional superstructures was named living polymers. Two different forces may favour the self-assembly of the system: Van der Waals and depletion interactions. The first one destabilize colloidal solution within time and the second depends linearly on the oleic acid concentration.[35]

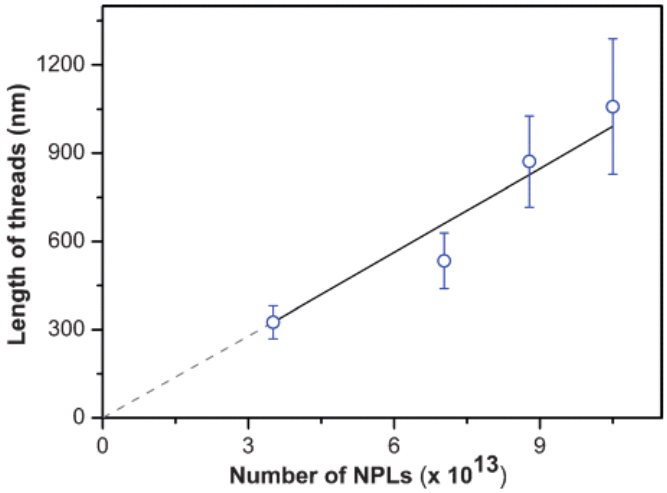

Figure 16. Dependence of the threads average length on the number of NPL added.

The gradual process of formation of stack of nanoplatelets was studied by Guzelturc *et al.*[36] They observed that the photoluminescence intensity decreases as the NPLs are formed into stacks upon addition of ethanol (Fig. 17).

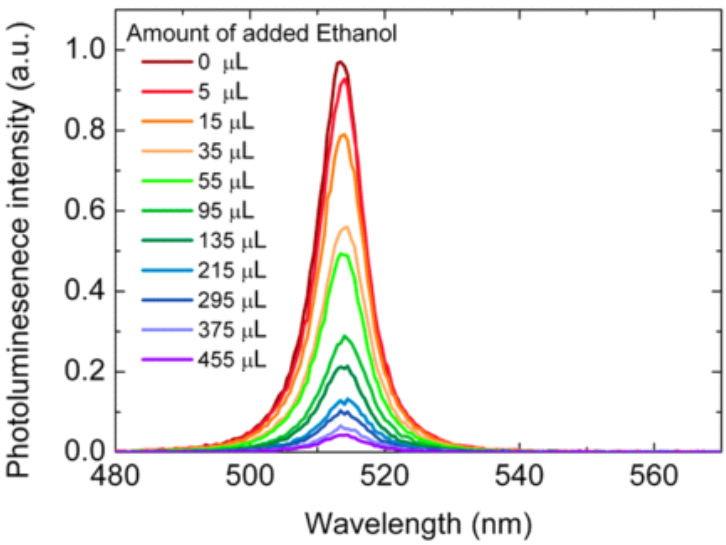

Figure 17. Influence of the stacking of NPLs on the fluorescence properties upon the addition of ethanol.

They showed that the quenching of the photoluminescence was linked to the existence of exciton migration. According to their explanation, the excitons migrate from one platelet to another within the stacked NPLs assemblies until they come to a non emissive well (Fig. 18). It has been reported that CdSe NCs bearing poorly passivated surfaces sites, crystal and surface defects can outcome in non-emmisive nanocrystals. For instance, hole trapping was associated to Cd vacancies and poor surface passivation in CdSe NCs leading to a non-radiative recombination of the exciton. Non-radiative recombination is when an electron in the conduction band recombines with a hole in the valence band and the excess of energy is emitted in the form of heat.[37] As a consequence, the existence of non-emissive platelets in stacked quantum wells can strongly decrease the photoluminescence intensity.[36]

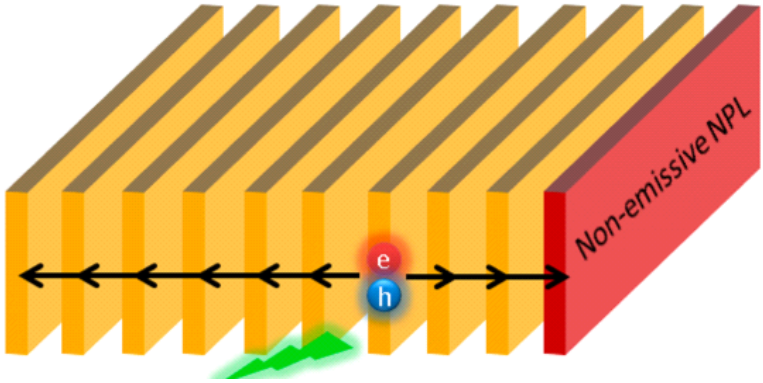

Figure 18. Scheme of nonemissive NPL within the stacks leading to hole trapping on the exciton migration, causing non radiative recombination which results in the photoluminescence emission decrease of the stacked NPLs.

In order to understand the influence of the nanocrystal environments, the spectroscopy of a single nanoplatele was analyzed at room temperature and at 20 K. Tessier et al. [38] compared the emission spectra of single CdSe NPLs on a glass surface in air with the emission of CdSe NPLs in solution. Surprisingly the emission spectrum of the single ones was very similar to the ones of unstacked ensembles (Fig. 19). This similarity is because there is no inhomogenous broadening in these ultrathin NPLs which is common detected for spherical and rodlike particles) and that is caused by size alteration. They also observed that the fwhm of single NPL is slightly bigger than the unstaked ensemble measurement. This behavior may be related to the fact that the single NPL were exposed in air which results in various emitting states. And these different emitting states may correspond to the rearrangements of the ligands as a consequence of the reversible interaction of the basal planes of the NPLs with H_2O and/or O_2 and photo-oxidation during illumination in air.[38]

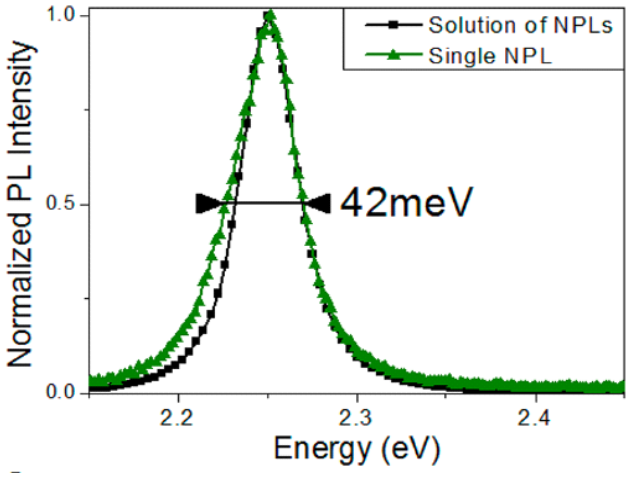

Figure 19. Emission spectra of NPLs in solution and on single platelet on a glass substrate at room temperature.

At 20 K, the fwhm of the PL spectrum of a single NPL decreases at low excitation, while the fwhm of the unstacked NPLs becomes larger (Fig. 20). The large inhomogenous broadening detected in unstacked nanoplatelets was related to spectral diffusion. Meaning that local variations of the enviroments can outcome in different emission maxima for every NPL.

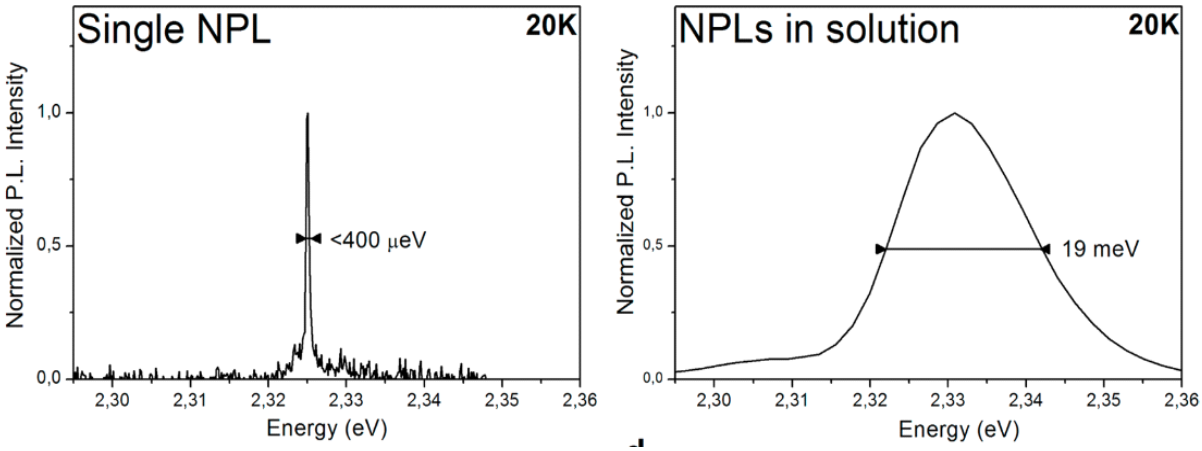

Figure 20. a) Emission spectra of a single NPLs (553 nm) and b) of an ensemble NPLs (553 nm) at 20 K.

Later the same authors[39] demonstrated that stacked NPLs show a different photoluminescence spectrum compared to the non-stacked ensembles at cryogenic temperatures. They exhibited the apparition of a second low energy line in the NPL self-assembly at 20 K (Fig. 21).

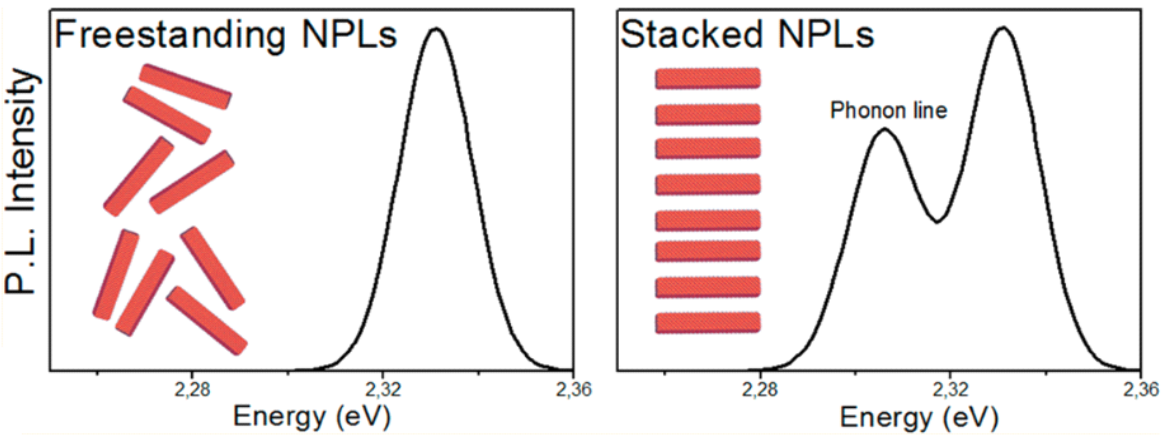

Figure 21. Emission spectra of dispersed NPLs (553 nm) (left) and stacked nanoplatelets at 20 K.

This red shifted emission line that begins to show up at 120 K was attributed to the phonon line-emission replica. According to their interpretation, a photon emitted in the main line (band edge transition) can be reabsorbed by neighbouring NPLs because the Stokes between the main line emission and the first absorption exciton is too small.

However, when the NPL emit the photon in the phonon line emission, the photon cannot be reabsorbed by stacked NPLs. The model proposed predicts the increase of the intensity of the phonon as the lateral dimensions of the NPLs increase, which explains why the phonon line emission is not observed when the NPLs are well dispersed or in single NPLs. In addition, the difference between the first and the second emission line is independent of the NPLs size, thickness, and surface ligand interaction. Interestingly, this energy gap is related to the character of the material (25 meV for CdSe and 20 meV for CdTe) (Fig. 22).[39]

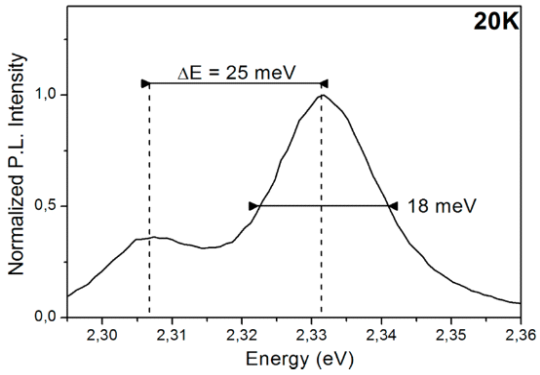

Figure 22. Emission spectra of an ensemble stacked NPLs (553 nm) demostrating the energy gap between the high energy line and the low energy line.

The NPLs optical properties are very much influenced by the environment (ligands, stacking, solvent, among other factors). It is both an advantage and a difficulty. Therefore we need to put attention to many parameters when preparing hybrids nanocrystals. At the same time optical spectroscopies can efficiently probe the correlations between the structure and the properties of such hybrid nanocrystals.

I. 8 References

1 A. L. Rogach, Semiconductor nanocrystal quantum dots, *Wien-New York Springer*.

2 A. M. Smith and S. Nie, Semiconductor Nanocrystals: Structure, Properties, and Band Gap Engineering, *Accounts Chem. Res.*, 2010, **43**, 190–200.

3 V. I. Klimov, *Semiconductor and Metal Nanocrystals: Synthesis and Electronic and Optical Properties*, CRC Press, 2003.

4 L. Cornejo, El porqué las diferentes propiedades de las nano partículas, http://nuevastecnologiasymateriales.com/el-porque-las-diferentes-propiedades-de-las-nano-particulas/, (accessed 2 April 2018).

5 A. Majid and M. Bibi, *Cadmium based II-VI Semiconducting Nanomaterials*, Springer International Publishing, Cham. 2018.

6 E. Cassette, PhD Thesis, Université Pierre et Marie Curie-Paris VI, 2012.

7 C. B. Murray, D. J. Norris and M. G. Bawendi, Synthesis and characterization of nearly monodisperse CdE (E = sulfur, selenium, tellurium) semiconductor nanocrystallites, *J. Am. Chem. Soc.*, 1993, **115**, 8706–8715.

8 S. Kar and S. Chaudhuri, Shape Selective Growth of CdS One-Dimensional Nanostructures by a Thermal Evaporation Process, *J. Phys. Chem. B*, 2006, **110**, 4542–4547.

9 Formation of ZnS nanostructures by a simple way of thermal evaporation, *J. Cryst. Growth*, 2003, **258**, 225–231.

10 J. Xu, J.-P. Ge and Y.-D. Li, Solvothermal Synthesis of Monodisperse PbSe Nanocrystals, *J. Phys. Chem. B*, 2006, **110**, 2497–2501.

11 Y. Li, H. Liao, Y. Ding, Y. Fan, Y. Zhang and Y. Qian, Solvothermal Elemental Direct Reaction to CdE (E = S, Se, Te) Semiconductor Nanorod, *Inorg. Chem.*, 1999, **38**, 1382–1387.

12 Y. Xie, D. Kocaefe, C. Chen and Y. Kocaefe, Review of Research on Template Methods in Preparation of Nanomaterials, *J. Nanomater.*, 2016, **2016**, 1–10.

13 M. Meyns, *Metal-semiconductor hybrid nanoparticles: Halogen induced shape control, hybrid synthesis and electrical transport*, Anchor Academic, 2014.

14 X. Peng and J. Thessing, in *Semiconductor Nanocrystals and Silicate Nanoparticles*, Springer, Berlin, Heidelberg, pp. 79–119.

15 Z. A. Peng and X. Peng, Nearly Monodisperse and Shape-Controlled CdSe Nanocrystals via Alternative Routes: Nucleation and Growth, *J. Am. Chem. Soc.*, 2002, **124**, 3343–3353.

16 Z. A. Peng and X. Peng, Mechanisms of the Shape Evolution of CdSe Nanocrystals, *J. Am. Chem. Soc.*, 2001, **123**, 1389–1395.

17 M. S. Bakshi, How Surfactants Control Crystal Growth of Nanomaterials, *Cryst. Growth Des.*, 2016, **16**, 1104–1133.

18 X. Peng, L. Manna, W. Yang, J. Wickham, E. Scher, A. Kadavanich and A. P. Alivisatos, Shape control of CdSe nanocrystals, *Nature*, 2000, **404**, 59–61.

19 A. Wolcott, R. C. Fitzmorris, O. Muzaffery and J. Z. Zhang, CdSe Quantum Rod Formation Aided By In Situ TOPO Oxidation, *Chem. Mater.*, 2010, **22**, 2814–2821.

20 Q. Pang, L. Zhao, Y. Cai, D. P. Nguyen, N. Regnault, N. Wang, S. Yang, W. Ge, R. Ferreira, G. Bastard and J. Wang, CdSe Nano-tetrapods: Controllable Synthesis, Structure Analysis, and Electronic and Optical Properties, *Chem. Mater.*, 2005, **17**, 5263–5267.

21 S. Ithurria and B. Dubertret, Quasi 2D Colloidal CdSe Platelets with Thicknesses Controlled at the Atomic Level, *J. Am. Chem. Soc.*, 2008, **130**, 16504–16505.

22 I. Fedin and D. V. Talapin, Colloidal CdSe Quantum Rings, *J. Am. Chem. Soc.*, 2016, **138**, 9771–9774.

23 Z. Li and X. Peng, Size/Shape-Controlled Synthesis of Colloidal CdSe Quantum Disks: Ligand and Temperature Effects, *J. Am. Chem. Soc.*, 2011, **133**, 6578–6586.

24 S. Ithurria, G. Bousquet and B. Dubertret, Continuous Transition from 3D to 1D Confinement Observed during the Formation of CdSe Nanoplatelets, *J. Am. Chem. Soc.*, 2011, **133**, 3070–3077.

25 M. Olutas, B. Guzelturk, Y. Kelestemur, A. Yeltik, S. Delikanli and H. V. Demir, Lateral Size-Dependent Spontaneous and Stimulated Emission Properties in Colloidal CdSe Nanoplatelets, *ACS Nano*, 2015, **9**, 5041–5050.

26 C. Bouet, M. D. Tessier, S. Ithurria, B. Mahler, B. Nadal and B. Dubertret, Flat Colloidal Semiconductor Nanoplatelets, *Chem. Mater.*, 2013, **25**, 1262–1271.

27 C. She, I. Fedin, D. S. Dolzhnikov, P. D. Dahlberg, G. S. Engel, R. D. Schaller and D. V. Talapin, Red, Yellow, Green, and Blue Amplified Spontaneous Emission and Lasing Using Colloidal CdSe Nanoplatelets, *ACS Nano*, 2015, **9**, 9475–9485.

28 S. Jana, T. N. T. Phan, C. Bouet, M. D. Tessier, P. Davidson, B. Dubertret and B. Abécassis, Stacking and Colloidal Stability of CdSe Nanoplatelets, *Langmuir*, 2015, **31**, 10532–10539.

29 E. Lhuillier, S. Pedetti, S. Ithurria, B. Nadal, H. Heuclin and B. Dubertret, Two-Dimensional Colloidal Metal Chalcogenides Semiconductors: Synthesis, Spectroscopy, and Applications, *Accounts Chem. Res.*, 2015, **48**, 22–30.

30 A. W. Achtstein, A. Antanovich, A. Prudnikau, R. Scott, U. Woggon and M. Artemyev, Linear Absorption in CdSe Nanoplates: Thickness and Lateral Size Dependency of the Intrinsic Absorption, *J. Phys. Chem. C*, 2015, **119**, 20156–20161.

31 E. Lhuillier, S. Pedetti, S. Ithurria, B. Nadal, H. Heuclin and B. Dubertret, Two-Dimensional Colloidal Metal Chalcogenides Semiconductors: Synthesis, Spectroscopy, and Applications, *Accounts Chem. Res.*, 2015, **48**, 22–30.

32 A. Antanovich, A. W. Achtstein, A. Matsukovich, A. Prudnikau, P. Bhaskar, V. Gurin, M. Molinari and M. Artemyev, A strain-induced exciton transition energy shift in CdSe nanoplatelets: the impact of an organic ligand shell, *Nanoscale*, 2017, **9**, 18042–18053.

33 B. Abécassis, M. D. Tessier, P. Davidson and B. Dubertret, Self-Assembly of CdSe Nanoplatelets into Giant Micrometer-Scale Needles Emitting Polarized Light, *Nano Lett.*, 2014, **14**, 710–715.

34 A. Hassinen, I. Moreels, K. De Nolf, P. F. Smet, J. C. Martins and Z. Hens, Short-Chain Alcohols Strip X-Type Ligands and Quench the Luminescence of PbSe and CdSe Quantum Dots, Acetonitrile Does Not, *J. Am. Chem. Soc.*, 2012, **134**, 20705–20712.

35 S. Jana, P. Davidson and B. Abécassis, CdSe Nanoplatelets: Living Polymers, *Angew. Chem. Int. Ed.*, 2016, **55**, 9371–9374.

36 B. Guzelturk, O. Erdem, M. Olutas, Y. Kelestemur and H. V. Demir, Stacking in Colloidal Nanoplatelets: Tuning Excitonic Properties, *ACS Nano*, 2014, **8**, 12524–12533.

37 A. Resnick, Introduction to Experimental Biophysics: Biological Methods for Physical Scientists, by Jay Nadeau, *Contemp. Phys.*, 2012, **53**, 379–379.

38 M. D. Tessier, C. Javaux, I. Maksimovic, V. Loriette and B. Dubertret, Spectroscopy of Single CdSe Nanoplatelets, *ACS Nano*, 2012, **6**, 6751–6758.

39 M. D. Tessier, L. Biadala, C. Bouet, S. Ithurria, B. Abecassis and B. Dubertret, Phonon Line Emission Revealed by Self-Assembly of Colloidal Nanoplatelets, *ACS Nano*, 2013, **7**, 3332–3340.

Chapter II: Dynamic assembly of CdSe nanoplatelets into superstructures

Chapter II: Dynamic assembly of CdSe nanoplatelets into superstructures

II. 1 Self-assembly

II. 1. 1 Concept

The origin of self-assembly dates back to 400 BC with the Greek philosopher Democritus, who imagined the organization of atomistic items to give life to the creation of the universe. Later in 1644, Descartes visualized the arrangement of small components to form larger associations driving by the chaos to explain the creation of an ordered universe. These two greatest philosophers in science inspired later many of the theories that point out the self-assembly process in the principal fields of science as chemistry, mathematics, physics, and biology.[1]

Self- means 'without outside help or on its own'. And *assembly* signifies 'to put together or even build'. Lately, Nature.com described assembly as the " the process by which an organized structure spontaneously forms from individual components, as a result of specific, local interactions among the components".[2] In other terms, self-assembly is a process by which different kinds of components such as atoms, molecules, colloids, and polymers spontaneously put themselves together to make complex structures through a broad variety of interactions.[3]

The description of assembly involves spontaneity. The basic building blocks or component interact between then to form structures in an ordered pattern from a disordered state. This process implies a high number of individual components ; for instance, crystallization may imply one mole or even more. In addition, structures can be formed in the three different dimensions (1D, 2D, and 3D).[4]

The process of self-assembly takes place either through static self-assembly or by dynamic self-assembly.

II. 1. 2 Types of assembly

Static assembly implies systems that are at equilibrium and it only occurs if the system is not dissipating energy.[5] In other terms, the building blocks assemble by reaching an energy minimum (equilibrium) to form ordered static equilibrium structures, in the absence of external forces.[1] Thus, the static equilibrium structures are stable once they are formed. Classic examples are liquid crystal, globular proteins, and nanoparticles[5].

On the other hand, a dynamic assembly in the presence of external influences involves systems that are out of thermodynamic equilibrium (known as dissipative systems), involving energy dissipation. In other words, dynamically assembled structures are formed thanks to a continuous energy supply. And when the influx of energy stops in the system, the structure disassembles.[1]

Nowadays, rules leading to static assemblies are well defined. Therefore, the biggest challenge to be overcome in the field is defining paradigms able to describe and predict out-of-equilibrium processes. And this relevance comes from the central role in life of dynamic processes. Indeed, any living organism is a dynamic system.[5]

Living systems consume energy from the environment while diminishing entropy. The energy is directed from the surrounding into the living structure by food or heating and when the energy stops the organism disassemble. Living organisms are made up of thousands of unit cells. And the cells die after the energy supply is interrupted. The cell is therefore a dynamic system. The role of the structures in the cell engages dynamic order such as filaments, histones, protein aggregates and chromatin.[1]

Non-living systems also experience dynamic organization. And unlike living systems, the non-living ones are less studied and understood.[5] In any case, both living and non-living systems comprise interacting components capable to adapt or react to the environment by the presence of chemical or physical influences.

Interestingly, some dynamically assembled systems spontaneously evolve into a higher level of complex patterns related to temporal gradients such as viscosity, temperature, pressure and chemical potential.

In general, the static assembly creates ordered structures that are in equilibrium. This system is permanent, but it can reach different equilibrium states when the surrounding changes[1]. On the contrary, in dynamic assembly the interacting components organize into complex structures and ordered patterns beyond of thermodynamic equilibrium. These structures are able to adjust to their environment when the system reorganizes by reaction to an external impulse. And these stable but out–equilibrium structures can be maintained or prevail only if there is a continuous supply of energy.[6] These systems come back to equilibrium once the supply of energy stops.[1]

The thermodynamic principles, kinetics and mechanism of self-oganization in nanostructures are intricate. The fundamentals of molecular thermodynamics may apply differently in nanosystems.[4]

In any case, self-assembly discloses to certain extent encrypted information in individual building blocks such as surface properties, shape, charge, magnetic dipole, which dictate the interaction between the system.[5]

The study of dynamic self-assembly phenomenon opens a path to understand the behavior of living dynamic system by mimicking nature in inanimate systems.

II. 1. 3 Assembly of nanoparticles

Years later after the discovery of the synthesis of nanoparticles, scientists detected the capacity of the nanocrystals to self-organize. Recently, we have seen a rapid growth in the area of the nanocrystals self-organization,[1] although not so many examples of assembled semiconducting nanocrystals are described.[7]

In nanoparticles assembly process, one of the most important physical necessities or even in other building blocks is the translational mobility. The mobility depends on the energy, and it is introduced by heat, magnetic field, electric field, mechanical deformations, light, etc.[8]

The assembly of nanoscale particles depends on different properties such as their size, aspect ratio, shape, solvents (also air), humidity, concentration and other environmental factors.[9]

Assembly involves specific interactions between the nanocrystals. And understanding and controlling these forces is a prerequisite to achieve the desired structures and functionalities. Thus, the first steps for a basic understanding is to recognize the diverse range and degree of strength of the internanoparticles forces.[9] These directional forces are Van der Waals forces, dipole-dipole interactions, steric repulsion caused by the surfactants monolayer, electrostatic interactions in apolar solvents and depletion interactions. For instance, Van der Waals forces are present in molecules and particles.[10] They are attractive when the materials are similar, but it may be repulsive when the materials are not similar, mostly in a liquid solvent. This interaction is strong on uncoated nanoparticles of metals, metal oxides, chalcogenides and ceramic materials, which induce the aggregation in non-polar medias.

On the other hand, it is known that the electrostatic interaction between particles can be either repulsive or attractive. If the particles are charged similarly this force is repulsive (in water).[9] Nevertheless, these interactions are less examined in non-polar medias. In non-polar solvents, the charges dissociate less easily. However, this doesn't mean that charges are not present.[10] On the contrary, the charges are weakly screened and such charges could induce a surface potential, which could have an effect over large distances. These interactions have been also responsible for the assembly of two nanoparticles of opposite signs in at liquid air interface.[10]

Moreover, steric repulsion (also known as steric stabilization) refers to nanoparticles that are coated with a monolayer of surfactant or polymers.[9] The surfactant layer provides colloidal stability through steric repulsion when the size of the nanocrystal is below 10 nm. But this stabilization can be complicated to achieve with larger nanoparticles (>20 nm).[11] Between the surfaces of nanoparticles, Van der Waals interactions are insignificant when comparing to repulsive steric forces. And the magnitude of these steric repulsion forces is more important for wires than for rods than for spheres.[9]

In addition, the repulsion between the colloidal nanocrystals depend on the ligand-solvent interaction, a poor solvent would decrease the repulsion and induce an assembly between nanocrystals.[10]

Depletion interactions[12] occur frequently in colloidal nanocrystals mixed with polymer chains or micelles. It has been defined by Vrij as "attraction through repulsion".

When two colloidal spheres become close, the depletion layer that surrounds the particles overlaps and the volume available for the polymers increases. The polymers excluded from the depletion space can push the nanocrystal to the other one, inducing an attractive force between them.

There are also interparticle forces that can emerge from external and internal forces. For instance, magnetic nanoparticles can undergo spontaneous self-assembly into rings without any external field, owing to the magnetic dipole-dipole nanoparticle interaction, but the application of the magnetic field can transform the organization into strings.[9] In the presence of an external electric field, the nanoparticles interact through similar dipole-dipole interaction, forming chains that are adjusted parallelly to the field, giving rise to well-ordered structures. Field-induced alignment was demonstrated for ligand-functionalized CdSe nanorods to form dense arrays of anisotropic nanocrystals.[9]

In order to control the assembly of nanoparticles, it appears clear that one has to control all these kinds of interactions. To trigger assembly it appears necessary to make one of these interactions dominate by applying a specific stimulus.[3]

II. 1. 4 Motivation of this work

This work was performed in collaboration with the group of Bio-inspired and Smart Materials led by Prof. N. Katsonis at the MESA+ institute for nanotechnology at the University of Twente. On the one hand, we could provide colloidal CdSe nanoplatelets and both of our groups knew about the work of Dubertret and Abécassis about the self-assembly of these objects by solvent evaporation or anti-solvent addition (see chapter 1). On the other hand, the Ph.D. subject of He Huang in Enschede dealt with "*azobenzenes as energy transducers in dynamic supramolecular systems*" and Katsonis's group is a world-leading group in converting light into motion in supramolecular systems. We therefore had the idea to convert light into motion in a supra-particular system by associating azobenzene molecules properties to NPLs. The problematic was to be able to use a remote stimulus (light) in order to trigger the assembly of NPLs into ribbons like Abécassis did with an internal stimulus.

To support our hypothesis, we considered the work of Klajn and coworkers[13] who demonstrated in 2007 that azobenzene moieties were capable to chemisorb on gold surfaces by a thiol functional group. More interestingly, these photoswitchable molecules could drive

the gold nanoparticles into aggregates using visible light and stabilized by dipole-dipole interactions between cis-azobenzene moieties. Considering the background of the colloidal CdSe nanoplatelets to present a strong tendency to assembly through interparticle interaction[10,14] and because their native ligands can be replaced by other ligands,[15,11] we decided to combine these photoswitchable molecules with CdSe nanoplatelets to induce their organization into structures.

We thank Prof. Nathalie katsonis for this collaboration and for welcoming me in her group twice and Dr. He Huang for helpful discussions and the synthesis of the azobenzene ligands at the University of Twente. I would like to acknowledge the *French-Dutch network for superior education and research* for financial support through the Eole fellowship and the *Michem* Labex for allowing me making these internships at the University of Twente.

II. 2 Azobenzenes

Unlike other energy sources, light offers an advantageous alternative for one of the biggest problems that the human society faces, which is the energy supply. Light allows a high spatial precision and does not produce any chemical waste.[16]

Optical switching feature in organic molecules is one of the most appealing targets of interest because of their future applications in energy storage systems or photochemical devices. Molecules photoswitches are molecules that use light to go through a reversible transformation between two states associated with different absorption/emissions properties.[17]

One of the most widely studied molecular photoswitches are the azobenzene derivatives. These organic molecules can go through a *trans*→*cis* isomerization when exposed to ultraviolet (UV) radiation. The *trans* isomer is almost planar and presents a dipolar moment close to zero. The *cis* form presents a bent structure with a dipolar moment of 3 Debye. The *trans* form can be regenerated in the dark, visible light or by heating. The *trans* isomer is more stable than the *cis* form and it can be produced with more than 99.99% in the dark.[18]

The absorption spectra of *trans* isomer display a strong absorbance signal near to λ = 320 nm, attributed to π-$\pi*$ transition and a weaker signal close to 440 nm referred to n-$\pi*$ band (figure 1). In the case of the *cis* isomer, a stronger absorbance band compared to the

trans isomer is found close to 440 nm, which corresponds to a n-π∗ transition, and two other weaker signals are found at 280 nm and 250 nm.[18]

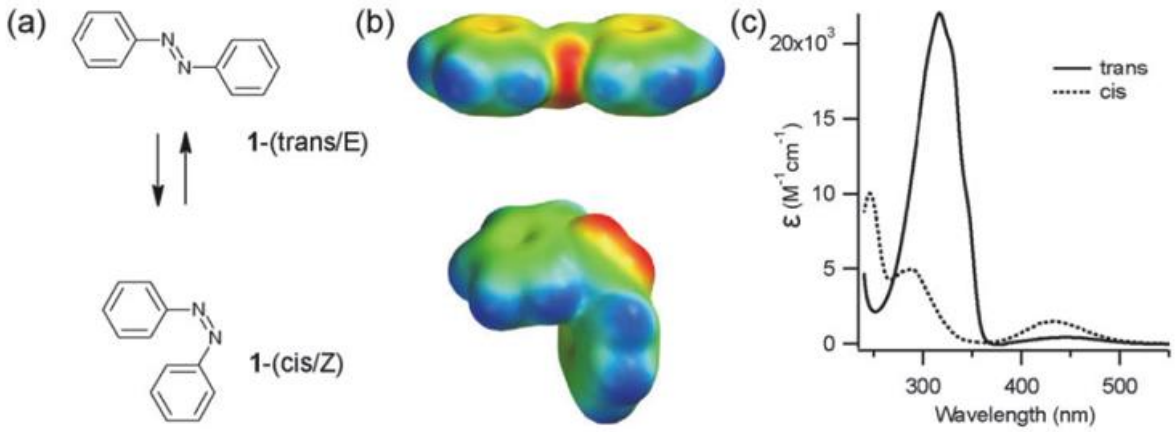

Figure 1. a) Structures of *trans* and *cis* configurations of azobenzenes, b) UV-Vis absorption spectra of *trans* and *cis* forms of azobenzene dissolved in ethanol.

Substituents on the phenyl rings could strongly modify the absorption bands of the azobenzenes, altering the light necessary to undergo the photoisomerization process. For instance, introducing the electron-donating methoxy groups at the *para* positions could red-shift the π-π∗ transition band of the azobenzene by 30 nm[19].

II. 3 Synthetic strategy

It has been reported that thiols are efficient stabilizing agents for II-VI semiconductors particles, such as CdS, CdTe and CdSe to provide monodispersity and stability.[20] The thiol groups are known to be the strongest ligands to the CdSe nanoparticles compared to phosphines and amines.[21] In addition, the ligand exchange between the native oleate ions of CdSe and the thiols is irreversible.[22] Hence, we decided to incorporate a thiol functional groups to the azobenzenes as capping ligands for the CdSe nanoplatelets.

We also intended to investigate the influence of the ligand chain on the assembly of the CdSe NPLs by coating the nanocrystals with azobenzenes bearing an alkyl chain of various lengths. The ligands chain could allow tuning the distance between nanoparticles once

assembled in order to tune in turn the optical properties of the stacks. Therefore, three azobenzenes have been selected. These molecules bear respectively a C3, a C11 and a C18 alkyl chain and will be refered as C3, C11 and C18 in the following (figure 2a). Derivatives bearing a tert-butyl group were also considered and will be named tBuC3, tBuC11 and tBuC18 in the following.

The azobenzenes were also designed with the electron-donating alkyloxy group in order to shift their absorption towards visible light. The *trans* and *cis* form of mono-methoxy azobenzene have dipole moments of respectively ~1.2 D and ~5 D.[23] Therefore we chose to work in chloroform since this solvent has a similar dipole moment (~1.2 D)[24] with respect to the *trans*-form. The UV/Vis absorption spectrum of the ligand C3 in its *trans*-isomer displayed a pronounced absorption band at 350 nm and a n-π transition band at λ = 440 nm (Fig. 2b). Upon irradiation with near UV light (λ = 365 nm) during 1 min, the intensity of the π-π* band strongly decreases; whereas the n-π* transition band increases, indicating *cis* isomerization. The *trans* configuration was regenerated 5 times upon visible irradiation, indicating that the system can be reversible (Fig. 2c).

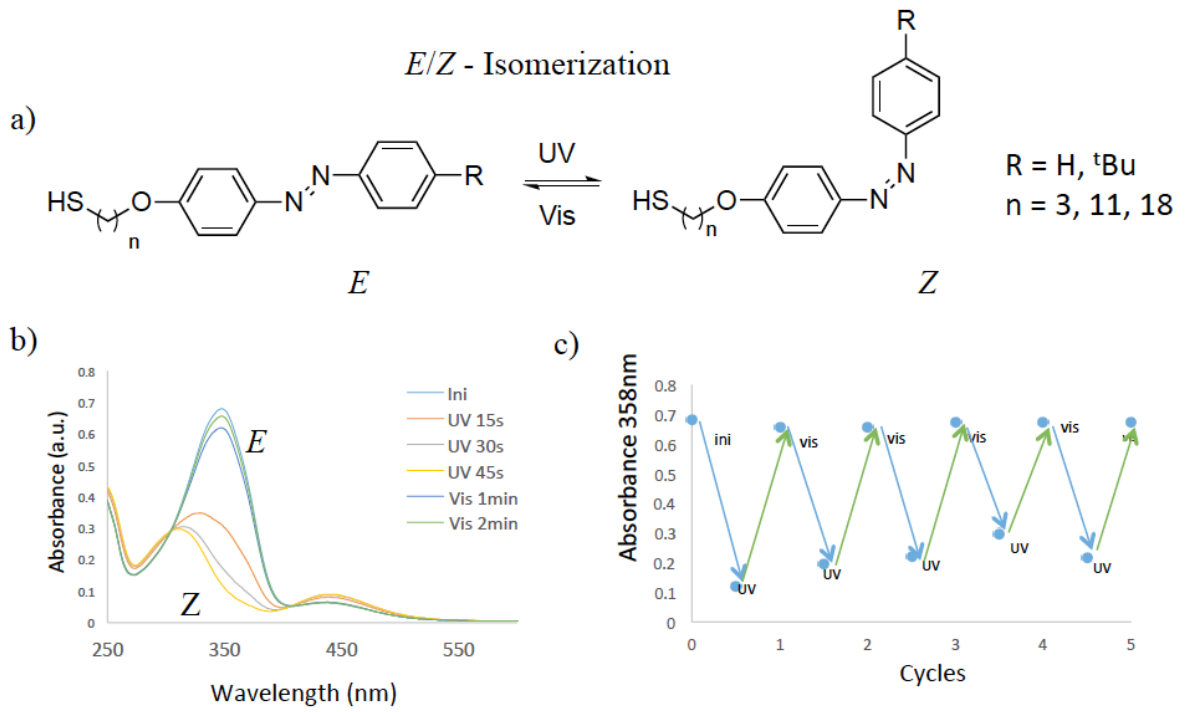

Figure 2. a) Structure of the azobenzene derivates switching between *trans* and *cis* configurations, b) Reversible changes in the UV/Vis spectra of the C3 ligand C3 (C = 70μM in chloroform) upon exposure to near UV light (λ = 365 nm) and visible light. d) Reversible cycles of the C3 ligand by using, respectively, UV and visible light.

II. 4 First generation of azobenzene ligands: C3, C11 and C18

II. 4. 1 CdSe nanoplatelets purification

The nanoplatelets emitting at 510 nm were sinthesized as it is mentioned in **annex A**. Then, the NPLs were isolated from platelets emitting at 460 nm, quantum dots, and other reaction by-products with selective precipitation/centrifugation steps. More precisely, the raw product was purified upon addition of hexane and ethanol (3:1 v/v ratio of hexane/ethanol) in an ultrasonic bath during 10 min. Then, the resulting mixture was centrifuged at 4000 rpm during 1 min, and the supernatant was discarded. The precipitate was finally dispersed in chloroform and the concentration of the 4 ML nanoplatelets was set at 5.08 nM.[25]

II. 4. 2 Ligand exchange

In a single neck flask, 2 mL of NPLs solution were introduced in 4 mL of chloroform and 0.5 mL of a solution of C3 ligand in chloroform (3.66×10^{-3} M). The mixture was heated to 70°C under argon atmosphere and vigorous stirring and kept at that temperature for 30 min. The reaction solution changed from yellow to orange suggesting NPLs functionalization. Then, the heating was stopped, and the reaction solution cooled to room temperature. The same reaction was done for C11 and C18. The solution was precipitated by the addition of ethanol and isolated by centrifugation and decantation to remove any excess unbound capping groups. The precipitate was finally redispersed in 2 ml of chloroform. After that, the solution was moved into a quartz cuvette, and characterizations were performed.

II. 4. 3 Results and discussion

In this work, we prepared ZB CdSe NPLs with a thickness of 4 MLs of lattice unit. The detailed synthesis method is described in chapter 1. Prior to treatment with azobenzene moieties, the NPLs were purified right after the synthesis. An excess of ligand was used, since it has shown that the ligand exchange of native oleate ligands on CdSe QDs was not reached unless an excess of exchanging ligands were used in the solution. In other terms, higher concentration of thiols induces faster exchange process.[26, 27] The solvent used for this work was chloroform because of the good colloidal stability of the nanocrystals and dipolar moment close to the *trans*-state of the azobenzene moieties.

Thiol is known to form strong[21,28] and irreversible[29] bonds with the surface of Cd ions of cadmium chalcogenide nanoparticles. These groups were reported to bind to the CdSe NCs surface in a X-type bonding between ligand anion and the surface of Cd^{2+} ion.[26] Also, previous studies have shown that neutral thiols first bind to free non-passivated sites before removing the native carboxylate ligands and binding then in form of thiolates ligands on the surface of CdSe QDs. The ligands substitution takes place through a proton exchange between ligands species and bound native carboxylate ion.[29,26] Taking into account that both top and bottom sides of the planes of ZB CdSe NPLs are representated by (100) plane, and terminated by Cd atoms,[30] we assumed the thiol ligand were attached to these planes (figure 3).

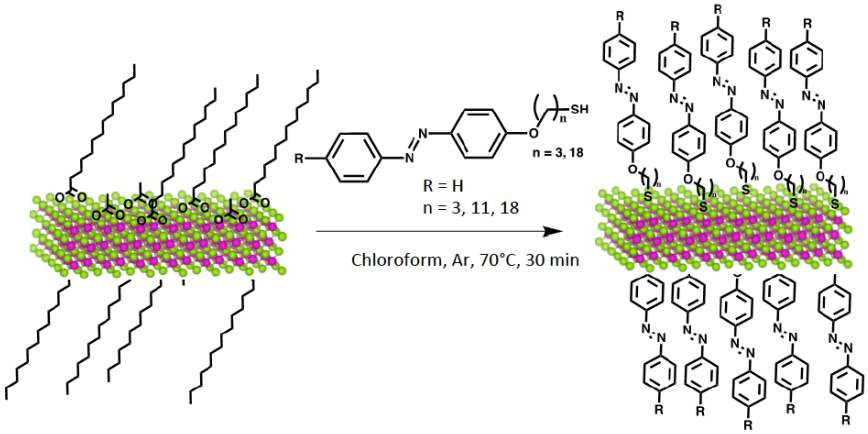

Figure 3: schematic depiction of the ligand exchange with azobenzenes derivates.

TEM images of CdSe NPLs coated with C3 dispersed in chloroform, and stored in darkness are shown on (figure 4a). The micrographs show that in the *trans*-state of the ligand C3, the solution presents both aggregated and individual NPLs. The latter are homogeneously dispersed and lay flat on the TEM sample substrate while the others are grouped in short stacks made up to 10 platelets with 4.6 nm in length and oriented perpendicular to the substrate. We also observe that the platelets are roughly nanodisk shapes with a lateral surface area of 420 nm on average, and a vertical thickness of 1.2 nm corresponding to 4 monolayers of CdSe nanoplatelets. We found that upon exposure to UV light, the nanoplatelets assembled into a long 1D-superstructure in an ordered manner instead of short stacks found in the trans-state (figure 4b). We interprate this result as follows: upon irradiation, the azobenzene ligands undergo the *trans-to-cis* isomerization leading to a change of their dipolar moment. In turn, the total dipolar moment of the NPLs is modified, triggering then their assembly into stacks.

The long superparticles oriented perpendicular to the plane of the nanocrystals can be as long as 500 nm and contain more than 100 nanoplatelets aligned face-to-face. The inter-NPLs distance has been measured to be approximately of 3.4 nm, the same distance as the one observed in the short stacks in the *trans*-form. At the same time, since this short-aggregation were found already before UV irradiation, it may be assumed that not all the original oleate ligands were removed by reaction with C3. However, this distance is slightly smaller than the one reported (~3.9 nm) for oleic acid molecules bound at the surface.[14,31] Therefore, a possible influence of the azobenzene in their *trans*-state to induce aggregation before irradiation must be considered. We supposed that π-π stacking of these molecules in their *trans*-state can occur between particles, inducing these short stacks.

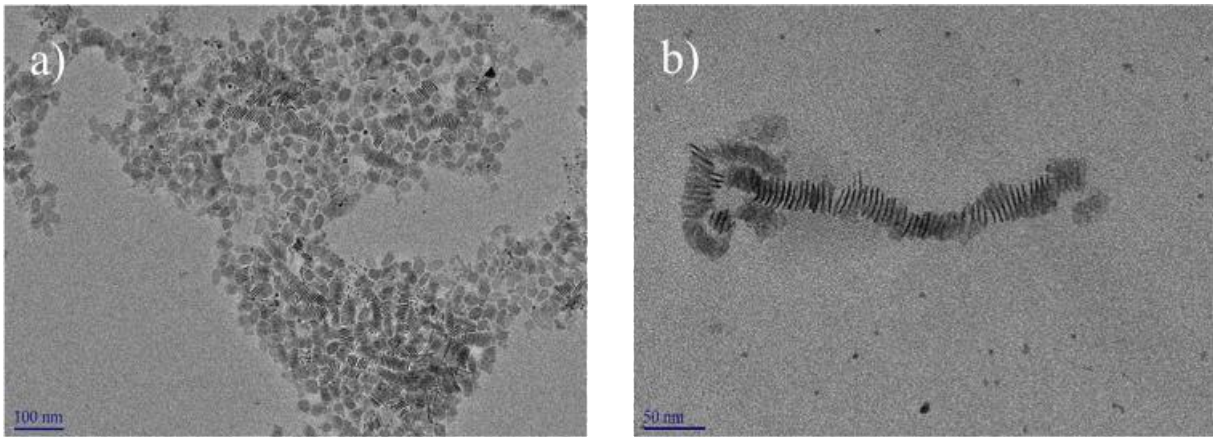

Figure 4: TEM images of CdSe NPls capped with C3 by ligand exchange before (a) and after UV illumination (b)

Based on these hypotheses, we decided to decorate the CdSe NPLs introducing a modification of the previous ligands by using a ^{t}Bu group in the para position of the azo group, which would create a steric hindrance that will forbid the π-π stacking between the *trans*-molecules.

We also decided to perform a treatment with $Cd(OAc)_2$ on the nanocrystal before functionalization, which induces the disaggregation of stacked NPLs generated by oleic acid.[26] In addition, this treatment replaces some surface oleates by acetates, providing a better steric availability to perform the ligand exchange.

II. 5 Second generation of azobenzene ligands: tBuC3, tBuC11, tBuC18

We carried out a series of treatment procedures in order to forbid any non-specific aggregation before iraadiation. First, the nanoplatelets were purified as described in the synthesis of hybrids C3/C11/C18. And then, the NPLS were treated before ligand exchange procedure by slightly modifying a previously reported treatment.[26]

II. 5. 1 NPLs treatment

Just after purification the precipitate was redispersed in 10 mL of octadecene and loaded into a three-neck flask with 40 mg of cadmium acetate (0.3 mmol) and 10 µl (0.1 mmol) of oleic acid. After degassing for 20 min, the mixture is heated to 150°C under an argon atmosphere during 10 min. Then, the heating mantle is removed and the reaction solution cooled to room temperature. The NPLs were precipitate with excess of ethanol and isolated by centrifugation at 9000 rpm for 5 min and decantation. The nanocrystals were finally redispersed in degassed chloroform and sonicated for 20 min.

II. 5. 2 Ligand exchange

The ligand exchange of native ligands with *t-Bu* azobenzenes was carried out analogously to previously mentioned. The same procedure was done for the three ligands tBu-(C3, C11, and C18). After functionalization each sample was precipitated out with ethanol, centrifugated at 9000 rpm during 5 min and the supernatant discarded. The precipitate was redispersed in previously degassed chloroform.

II. 5. 3 Results and discussion

During our experiments, we noticed that the treatment of the NPLs with $Cd(OAc)_2$ leads to a faster ligand exchange. Upon the treatment, the acetate ion displaces some of the oleate ions bounded to the surface, decreasing the ligand-ligand interaction, thus favoring NPLs disaggregation. At the same, this steric repulsion between nanocrystals will provide a better steric availability to induce an efficient ligand exchange. We also noted that in comparison to C3, the functionalization with tBuC3 resulted in a clearer solution indicating the improvement of the colloidal stability of the system.

In addition, we also examined the effect of the thiol ligand on the optical properties of the CdSe NPLs. On figure 5 the absorption spectra of CdSe nanoplatelets before and after ligand exchange of carboxylate ions with thiol ligands are presented. The ligand exchange induced considerable redshifting of both absorption bands electron/heavy hole (~ 26 nm) and electron/light-hole (~21 nm). This redshift may suggest the successful ligand exchange procedure. In addition, such large redshifting (10-40 nm) has been confirmed for capping ligands such as aliphatic thiols coating QDs[26] and more recently CdSe NPLs.[26,31] The latter[15] was related to a ligand-induced strain that changes the NPLs thickness; in other terms, a distortion of the unit cell altering the excitonic band gap of CdSe semiconductors. The redshift could also indicate no oxidation during the NPLs/azobenzene treatment. Oxygen contributes to the formation of CdO layer on the platelet surface,[11] and oxidation has been visible as a blue-shift for QDs in the UV-Vis absorption.[32]

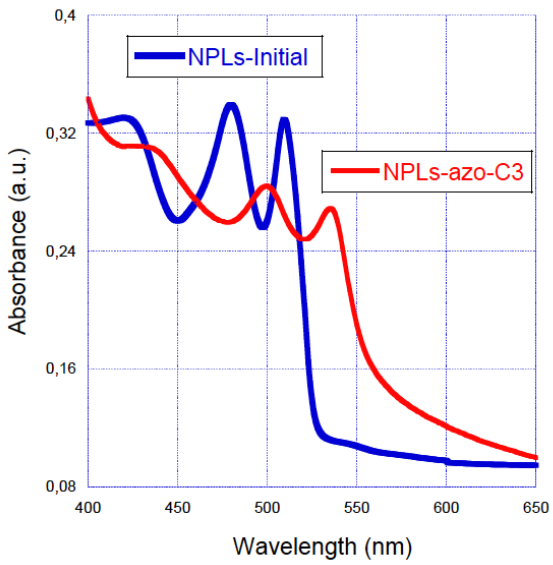

Figure 5. Absorption espectrum of CdSe nanoplateletes prior (blue) and after (red) ligand exchange with azo-C3

We also studied by dynamic light scattering (DLS) the solutions of modified NPLs and we did a comparison between NPLs-C3 and NPLs-tBuC3 prior to and after UV illumination (table 1). Initially, the NPLs-C3 presents a hydrodynamic diameter of 110 nm. But after 1 min of illumination at 365 nm, the average hydrodynamic diameter increases to 545 nm, suggesting an aggregation of the NPLs. Such aggregation is partially reversible since,

after relaxation, the diameter decreases back to 212 nm. However, the system improves after decorating the NPLs with ^{t}BuC3, as it can be noticed that in their initial state the hydrodynamic average size of the nanoparticles decreases, meaning that using ^{t}*Bu* group can greatly improve the dispersibility of the particles in chloroform. In addition, upon UV illumination the hydrodynamic average size of the particles increases thanks to the photoswitchable ligands, and the system comes back to its initial state once the supply of UV light is stopped. The UV illuminations were displayed one more time to reveal an efficient reversible-stacking process.

This behavior noticed in DLS measurements is consistent with the one observed on TEM images. The initial state of NPLs/^{t}*Bu*-C3 (figure 6a) does not show the presence of small stacks, instead, the NPLs exhibit a better dispersibility with random orientation in comparison to the one with C3.

C3			tBuC3		
step	size (nm)	+/− (nm)	**step**	size (nm)	+/− (nm)
initial	110	13	**initial**	26	4
1 min @ 365 nm	545	53	**1 min @ 365 nm**	425	150
5 min @ visible	212	26	**5 min @ visible**	58	20
1 min @ 365 nm	616	60	**1 min @ 365 nm**	375	100

Table 1. DLS measurements of NPLs functionalized by C3 and tBuC3 before and after UV irradiation.

The initial good dispersity of the NPLs is explained by the effect of the ^{t}Bu group that restrict the π-π stacking between the *trans* molecules attached to the NPLs surface. This observation also excludes the tendency for aggregation due to drying process on the TEM grids. Notably, upon irradiation at 365 nm, the nanoplatelets assemble into 1D ultralong ordered microstructures (Fig. 6b).

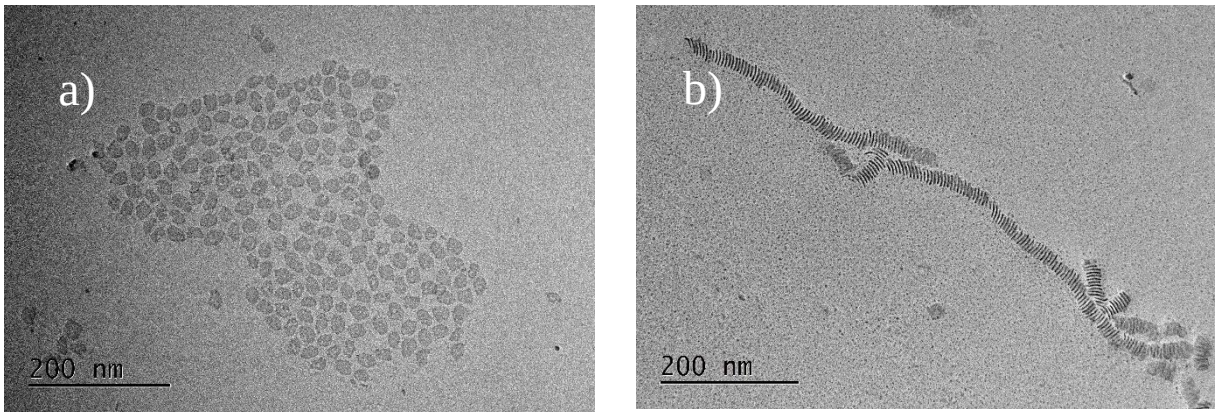

Figure 6: TEM images of CdSe NPLs functionalized with *t-bu* group a) before and b) after illumination at 365 nm.

This suggests that the *trans→cis* isomerization of the molecule induced a highly ordered microstructure triggered by an increase of the dipolar moment as the driving force for the assembly of NPLs (figure 7). These ultra long-assemblies were found to be as long as 1 µm composed of 200 nanoplatelets in a stack.

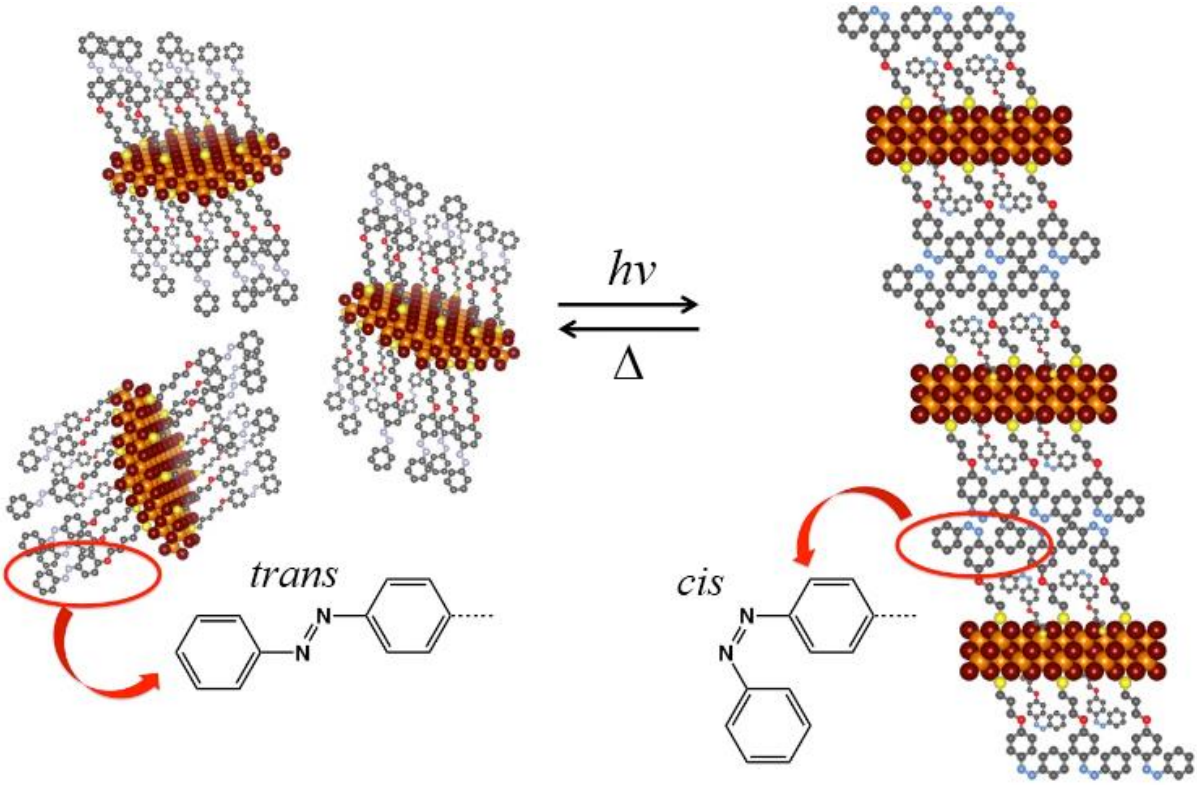

Figure 7: Schematic representation of the out-equilibrium face-to-face assembly of azobenzene-decorated CdSe NPLs: assembly of CdSe NPLs upon UV irradiation (λ = 365 nm, cis-state) and dissambly (trans-state) upon relaxation.

As we can see, the NPLs demonstrate a strong tendency to pack face-to-face rather than side-to-side. To explain this phenomenon, we have to mention that the nanoplatelets compared with QDs, exhibit very high surface area and lower surface curvature. The larger area of interaction promotes a more efficient assembly, and the low curvature enhances the ligand-particle interface and interparticle interaction. All these factors may contribute to the face-to-face assembly rather than side-to-side to form nanosheets. However, upon closer examination we can find some columns aligned close to each other indicating a possible interparticle interaction, this could be explained by the fact that lateral edges are composed of Cd and Se and the Cd are bind to thiol ligands (figure 8 a, b).

In order to understand the influence that the ligands have on the assembly of the nanoparticles we varied the length of the molecules. Although the functionalization with ^{t}*Bu*-C11 could not be obtained, the decoration with ^{t}*Bu*-C18 revealed the same tendency upon UV irradiation with some differences. In this case the superstructures did not align close to each other, instead they were crossed like forming a network configuration (figure 8 c, d).

Surprisingly, we find that the distance between assembled nanoplatelets is the same (3.4 nm) in all cases, no matter the length of the ligand. A possible reason may be the presence of some oleic acids that were not removed. Since the theoretical length of oleic acid molecules is 2.5 nm we suspect that alkyl chains could be collapsed or interdigitated.[14] Therefore, oleic acid could dictate the distance between the nanoparticles.

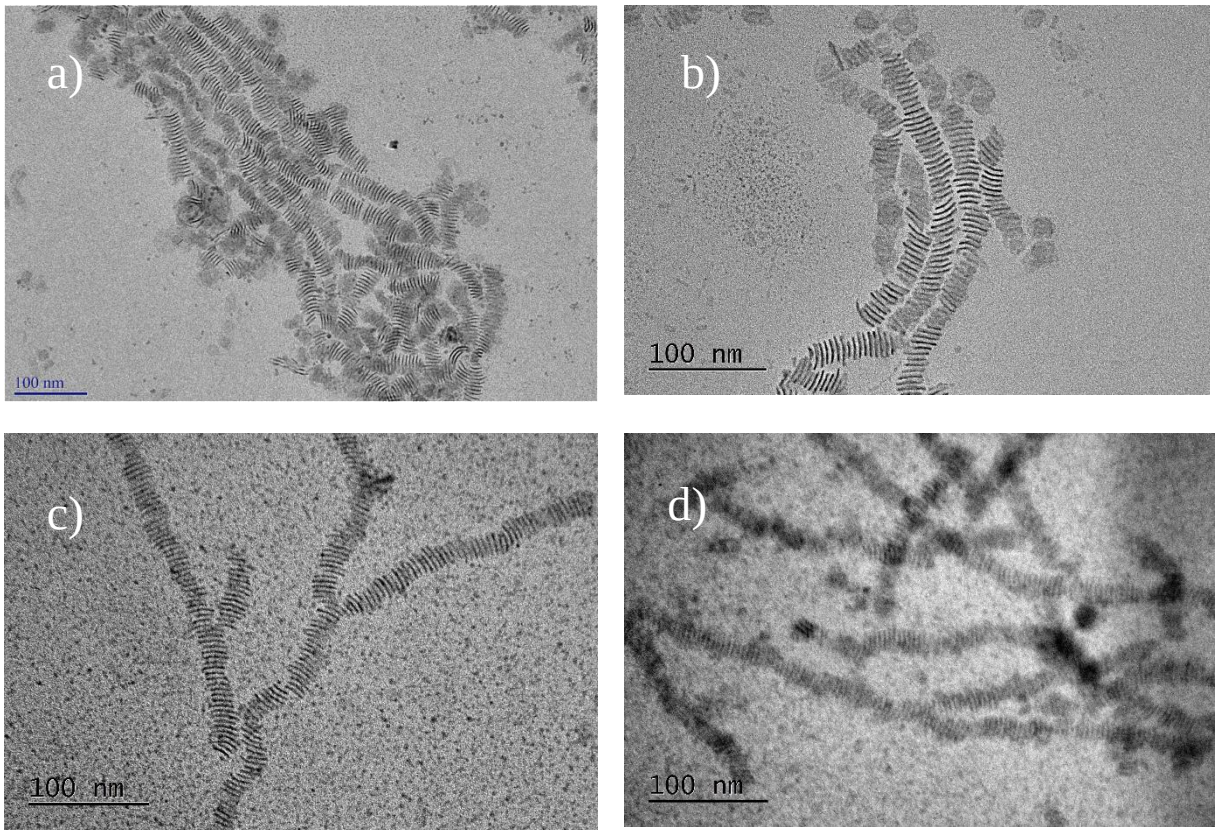

Figure 8. TEM images of CdSe NPLs functionalized with azobenzenes molecules upon near UV illumination a) NPLs/azo-C3, b) NPLs/t-bu-C3, c) and d) NPLs/t-bu-C18.

In conclusion, exposure to UV light triggers the assembly of CdSe nanoplatelets, as demonstrated by TEM analysis. Also, DLS indicated that this out-equilibrium system remains unaffected as long as there is a continuous influx of energy into the system. And all these features represent a dynamic assembly process rather than a static assembly.

II. 6 Conclusion and outlooks

We presented in this work the ligand exchange reactions at CdSe NPLs surface using azobenzenes molecules with a surface-anchoring group (thiol).

We demonstrated that the photoisomerization of the azobenzene molecules, upon UV illumination drives NPLs into long aligned filaments. The UV illumination can yield the transition of these molecules from their stable *trans* state into *cis* state to induce the attraction between nanoparticles.

By means of DLS, we also probed that covering the NPLs with a modification of the ligand, in our case, incorporating a ^{t}Bu group on the para position of the azo group, the dispersibility of the nanoparticles improves because it creates a steric hindrance that forbids the π-π stacking in the trans-state of the molecule. More importantly, we demonstrated that the system is reversible when the influx of UV illumination is stopped.

The current observations in absorption measurements are consistent with the one previously reported, suggesting the ligand exchange of oleic acids with thiol ligand. Aditionally, the interparticle distance may suggest the presence of native oleic acids that were not removed.

The CdSe NPLs were able to organize into long threads under external impulse like the dipole-dipole interactions in the *cis* for of the molecule, which is the driving force to form the assembly of these nanocrystals. The out-equilibrium superstructures were maintained when there was a continuous dissipation of energy. These conditions lead us to believe a possible dynamic assembly of the nanoparticles.

One of the questions we should address in order to examine the functionality of the system is; are the optical properties tuned by the assembly of the nanoparticles? Since we have not seen any significant change in the photoluminescence emission at room temperature, further tests will aim at low temperature to verify the possible presence of the phonon replica line previously observed in NPLs stacks (chapter 1).

A comprehensive study of the nanoparticles assembly kinetics could also be achieved through *in-situ* fluorescence microscopy. This will give us information about the assembly mechanism, to investigate whether the new NPLs join to already existing filaments or if the existing filaments join to each other to form a new existing one.

II. 7 Methods

Dynamic light scattering (DLS)

DLS measurements were carried out using a Malvern Zetasizer with a 532 nm excitation source. To measure the aggregation *in situ*, the solution was previously sonicated for 30 min, kept in dark at room temperature. Afterward, the mixture was irradiated at UV (λ = 365 nm) for 1 min in the zeta sizer using an optic fiber and the size was measured. Then, the solution was exposed to ambient light for 5 min and again illuminated under UV irradiation for 1 min, and the size was measured again.

UV-Vis spectra

The solution was precipitated by the addition of ethanol and isolated by centrifugation and decantation to remove any excess unbound capping groups. The precipitate was finally redispersed in 2 ml of chloroform. The UV-Vis spectra were recorded on a Jasco absorption spectrophotometer at room temperature, using 1 cm path length quartz cells. The absorbance value of the hh-e transition band of the initial NPLs was used to calculate the molar particle extinction coefficient and so the concentration of the nanoplatelets using empiric formulas depending on the lateral size.

Transmission electron microscopy

TEM images were performed by using a Tecnai spirit G2 cryomicroscope operating at an acceleration voltage of 120 kV. TEM images are recorded by Patrick Le Griel at LCMCP. TEM samples were prepared by depositing a droplet of the nanoparticles dispersion on a copper grid coated with a carbon film and letting it dry in the darkness for one night before the observation. The recordings were taken before (keeping the sample in darkness) and after 365 nm illumination.

II. 8 References

1 G. A. Ozin, K. Hou, B. V. Lotsch, L. Cademartiri, D. P. Puzzo, F. Scotognella, A. Ghadimi and J. Thomson, Nanofabrication by self-assembly, *Mater. Today*, 2009, **12**, 12–23.

2 Self-assembly, https://www.nature.com/subjects/self-assembly?WT.ac=search_subjects_self_assembly, (accessed 23 July 2018).

3 M. Grzelczak, J. Vermant, E. M. Furst and L. M. Liz-Marzán, Directed Self-Assembly of Nanoparticles, *ACS Nano*, 2010, **4**, 3591–3605.

4 G. M. Whitesides, J. K. Kriebel and B. T. Mayers, in *Nanoscale Assembly*, Springer, Boston, MA, 2005, pp. 217–239.

5 G. M. Whitesides and B. Grzybowski, Self-Assembly at All Scales, *Science*, 2002, **295**, 2418–2421.

6 J. V. I. Timonen, M. Latikka, L. Leibler, R. H. A. Ras and O. Ikkala, Switchable Static and Dynamic Self-Assembly of Magnetic Droplets on Superhydrophobic Surfaces, *Science*, 2013, **341**, 253–257.

7 M. A. Boles, M. Engel and D. V. Talapin, Self-Assembly of Colloidal Nanocrystals: From Intricate Structures to Functional Materials, *Chem. Rev.*, 2016, **116**, 11220–11289.

8 N. A. Kotov, Self-assembly of inorganic nanoparticles: Ab ovo, *EPL Europhys. Lett.*, 2017, **119**, 66008.

9 Y. Min, M. Akbulut, K. Kristiansen, Y. Golan and J. Israelachvili, The role of interparticle and external forces in nanoparticle assembly, *Nat. Mater.*, 2008, **7**, 527.

10 B. Abécassis, Three-Dimensional Self Assembly of Semiconducting Colloidal Nanocrystals: From Fundamental Forces to Collective Optical Properties, *ChemPhysChem*, 2016, **17**, 618–631.

11 S. Jana, T. N. T. Phan, C. Bouet, M. D. Tessier, P. Davidson, B. Dubertret and B. Abécassis, Stacking and Colloidal Stability of CdSe Nanoplatelets, *Langmuir*, 2015, **31**, 10532–10539.

12 H. N. W. Lekkerkerker and R. Tuinier, *Colloids and the depletion interaction*, Springer, Dordrecht ; New York, 2011.

13 R. Klajn, K. J. Bishop and B. A. Grzybowski, Light-controlled self-assembly of reversible and irreversible nanoparticle suprastructures, *Proc. Natl. Acad. Sci.*, 2007, **104**, 10305–10309.

14 B. Abécassis, M. D. Tessier, P. Davidson and B. Dubertret, Self-Assembly of CdSe Nanoplatelets into Giant Micrometer-Scale Needles Emitting Polarized Light, *Nano Lett.*, 2014, **14**, 710–715.

15 A. Antanovich, A. W. Achtstein, A. Matsukovich, A. Prudnikau, P. Bhaskar, V. Gurin, M. Molinari and M. Artemyev, A strain-induced exciton transition energy shift in CdSe nanoplatelets: the impact of an organic ligand shell, *Nanoscale*, 2017, **9**, 18042–18053.

16 M.-M. Russew and S. Hecht, Photoswitches: From Molecules to Materials, *Adv. Mater.*, 2010, **22**, 3348–3360.

17 N. Withers, Molecular photoswitches: The worm that turned off, *Nat. Chem.*, 2010, **2**, 11.

18 A. A. Beharry and G. A. Woolley, Azobenzene photoswitches for biomolecules, *Chem. Soc. Rev.*, 2011, **40**, 4422.

19 D. Manna, T. Udayabhaskararao, H. Zhao and R. Klajn, Orthogonal Light-Induced Self-Assembly of Nanoparticles using Differently Substituted Azobenzenes, *Angew. Chem. Int. Ed.*, 2015, **54**, 12394–12397.

20 A. Eychmüller and A. L. Rogach, Chemistry and photophysics of thiol-stabilized II-VI semiconductor nanocrystals, *Pure Appl. Chem.*, 2000, **72**, 179–188.

21 A. C. Wisher, I. Bronstein and V. Chechik, Thiolated PAMAM dendrimer-coated CdSe/ZnSe nanoparticles as protein transfection agents, *Chem. Commun.*, 2006, 1637.

22 R. R. Knauf, J. C. Lennox and J. L. Dempsey, Quantifying Ligand Exchange Reactions at CdSe Nanocrystal Surfaces, *Chem. Mater.*, 2016, **28**, 4762–4770.

23 H. Akiyama, K. Tamada, J. Nagasawa, K. Abe and T. Tamaki, Photoreactivity in Self-Assembled Monolayers Formed from Asymmetric Disulfides Having para-Substituted Azobenzenes, *J. Phys. Chem. B*, 2003, **107**, 130–135.

24 Bansal, *Organic Reaction Mechanisms*, Tata McGraw-Hill Education, 1998.

25 A. Yeltik, S. Delikanli, M. Olutas, Y. Kelestemur, B. Guzelturk and H. V. Demir, Experimental Determination of the Absorption Cross-Section and Molar Extinction Coefficient of Colloidal CdSe Nanoplatelets, *J. Phys. Chem. C*, 2015, **119**, 26768–26775.

26 A. Antanovich, A. Prudnikau, A. Matsukovich, A. Achtstein and M. Artemyev, Self-Assembly of CdSe Nanoplatelets into Stacks of Controlled Size Induced by Ligand Exchange, *J. Phys. Chem. C*, 2016, **120**, 5764–5775.

27 B. Fritzinger, R. K. Capek, K. Lambert, J. C. Martins and Z. Hens, Utilizing Self-Exchange To Address the Binding of Carboxylic Acid Ligands to CdSe Quantum Dots, *J. Am. Chem. Soc.*, 2010, **132**, 10195–10201.

28 B. C. Sih and M. O. Wolf, CdSe Nanorods Functionalized with Thiol-Anchored Oligothiophenes, *J. Phys. Chem. C*, 2007, **111**, 17184–17192.

29 R. R. Knauf, J. C. Lennox and J. L. Dempsey, Quantifying Ligand Exchange Reactions at CdSe Nanocrystal Surfaces, *Chem. Mater.*, 2016, **28**, 4762–4770.

30 R. S. Koster, C. Fang, A. van Blaaderen, M. Dijkstra and M. A. van Huis, Acetate ligands determine the crystal structure of CdSe nanoplatelets – a density functional theory study, *Phys. Chem. Chem. Phys.*, 2016, **18**, 22021–22024.

31 M. D. Tessier, L. Biadala, C. Bouet, S. Ithurria, B. Abecassis and B. Dubertret, Phonon Line Emission Revealed by Self-Assembly of Colloidal Nanoplatelets, *ACS Nano*, 2013, **7**, 3332–3340.

32 A. P. Alivisatos, Semiconductor Clusters, Nanocrystals, and Quantum Dots, *Science*, 1996, **271**, 933–937.

Chapter III: Composite materials made of CdSe nanoplatelets and metallophthalocyanines

Chapter III: Composite materials made of CdSe nanoplatelets and metallophthalocyanines

In the previous chapter we demonstrated the assembly of the CdSe NPLs mediated by azobenzene ligands. The azobenzene ligands were grafted on the surface of CdSe NPLs and exposed to UV irradiation, inducing the functional *cis*-isomer of the ligand. The *cis* isomer of the azobenzenes allows dipolar-dipolar interactions between azo groups, triggering the NPLs assembly. The system was shown to be also reversible after been exposed to visible light.

The formation of these NPLs assemblies opened up the possibility to extend this idea by introducing interesting coordination complexes leading to the tailoring of the magnetic and optical properties of the resulting composite material. To do so, we decided to use metallophthalocyanine complexes that have specific optical properties as well. Their optical and magnetic properties are dictated by the valence and spin state of the transition metal ion. This feature is in particular true for the cobalt (II) phthalocyanine (CoPc), which is the subject of this chapter.

III. 1 Phthalocyanines

III. 1. 1 Structures

Phthalocyanines, usually abbreviated as H_2Pcs, are macrocyclic ligands. Their structure is given on figure 1a. They bear a 18-π-electrons aromatic system, containing 4 isoindole subunits connected by four aza (-N=C-) groups at the α position of each isoindole. Phthalocyanines are structurally related with the macrocyclic ring system of porphyrins.[1]

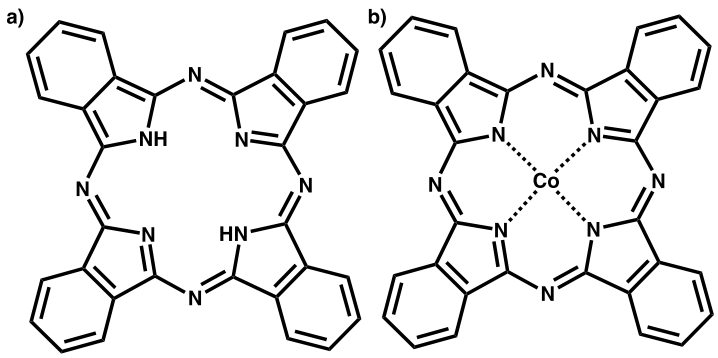

Figure 1. Chemical structure of H_2Pc (a) and CoPc (b)

Phthalocyanines exhibit a central cavity to incorporate different metal ions. This molecule can form complexes with 70 different metal ions, which influences its physical properties.[2] Therefore, the phthalocyanine exists as a dianion Pc^{2-} when a metal of oxidation state +II (Cu^{2+}, Co^{2+} and Fe^{2+}) is introduced into the macrocycle. Up to two electrons can be released from the Pc molecules and four electrons can be added. In other terms, the Pc oxidation states can go from Pc(0) (oxidized species) to Pc (-VI) (reduced species).[3] The Pc ring exhibits a planar structure, but the character of the central metal atom can affect the bond lengths and angles.[4] Some metal ions are too large to fit well into Pc ring, generating a distortion of the planar structure of the macrocycle. Nevertheless, we focus in this chapter on Co(II)Pc for which the Co^{2+} ion accommodates well in the Pc ring (figure 1b).

III. 1. 2 Solubility issues

Unsubstituted metal phthalocyanines have very poor solubility in common solvents. This is either due to strong π–π stacking or metal-metal interaction in the case of MPcs bearing an unpaired electron in the d_{z2} orbital (such as CoPc). Therefore, many studies target the synthesis of pheripheral substituted phthalocyanines bearing hydrocarbon chains or bulky groups that could improve the solubility of the compound.[2]

The synthesis of such molecules can be extremely time demanding, therefore we focused on commercially available unsubstituted Pcs. Ghani and coworker[5] investigated the solubility of unsubstituted metal phthalocyanines in a series of conventional solvents, acids and ionic liquids. They found that MgPc and ZnPc exhibit the highest solubility and their solutions are long-term (weeks) stable at ambient atmosphere. In contrast, FePc, MnPc and CoPc dissolve but only at reasonable concentrations (*i.e.* FePc: 1.25 $\times 10^{-5}$, MnPc: 6.62 x 10^{-3} and CoPc: 9.87 x 10^{-5} in THF) and they are not very stable if exposed to oxygen and light since the metal ion can oxydize. When it comes to CuPc, NiPc and SnPc, they have a very poor solubility. As a consequence we focused our study on CoPc since it is paramagnetic, reasonably stable (synthesis have nevertheless been performed in the dark) and reasonably soluble in THF.

III. 1. 3 Electronic properties of cobalt phtalocyanine

An understanding of the typical UV-visible spectra of Pcs and MPcs (mercaptopyridines) could be a prerequisite to the interpretation of the structure of the composite materials described in this chapter. Indeed, the very large molar absorption coefficient of Pcs and MPcs allows UV-visible studies of composites embedding low quantities of CoPcs. Therefore, we will briefly describe here the electronic absorption spectra of CoPcs depending on the presence of an apical ligand on the Co^{2+} ion. The formation of $[CoPc(MP)_2]$ might take place through an axial ligand exchange reaction of THF by MP (4-mercaptopyridine) onto CoPc. Nyokong[6] demonstrated that the formation of $[CoPc(py)_2]$ complexes in DMSO occurs in different steps by dissociation and under equilibrium. In analogy to this hypothesis, we propose that the $[CoPc(MP)_2]$ is produced by the substitution of the first axial THF ligand by MP. According to the author, the substitution of the first axial ligand is much faster than the second one.

$$MP + [CoPc(THF)_2] = [CoPc(THF)(MP)] + THF \quad (1)$$

$$MP + [CoPc(THF)(MP)] = [CoPc(MP)_2] + THF \quad (2)$$

The UV-visible spectrum of CoPc in THF is given on figure 2a (red). On this spectrum one can identify an intense band at 656 nm, called Q band. The sharp and intense Q band typically corresponds to a $\pi \rightarrow \pi^*$ transition from the HOMO to the LUMO. The second band in the UV region of the spectrum, called Soret or B band, corresponds also to a $\pi \rightarrow \pi^*$ transition that takes place from a deeper π orbital to the LUMO.

Introduction of an apical 4-mercaptopyridine (MP) ligand to CoPc has been monitored by UV-visible spectroscopy (figures 2a and 2b for magnification). When the molar ratio of CoPc to MP is 1:1, we notice that the maximum of the Q-band is not affected by the addition of the MP apical ligand (the later presenting an absorption band at 360 nm not observable on the adduct).

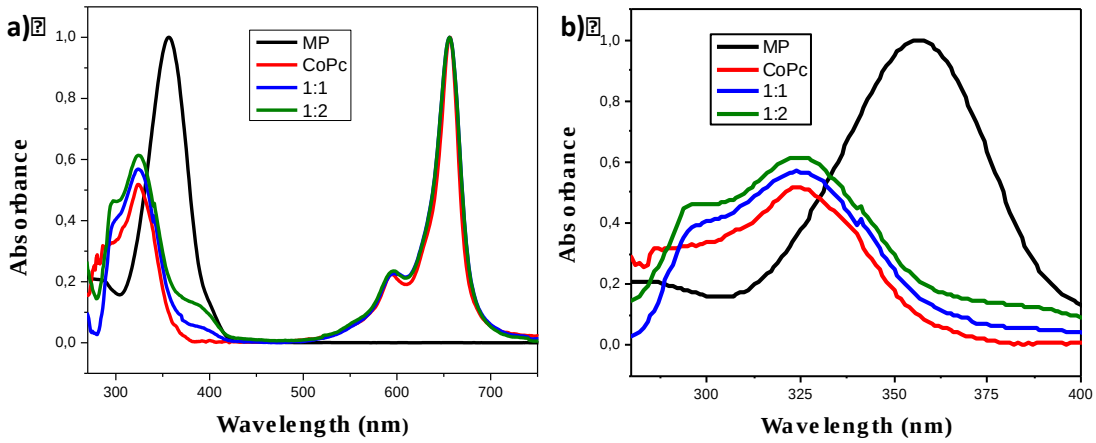

Figure 2: (a) UV-visible spectra of CoPc in THF (red) and evolution of this spectrum upon addition of a 1:1 (blue) and 1:2 (green) molar ratio of MP; (b) magnification of these spectra in the region of the B band. The spectrum of MP in THF (black) is also given.

In contrast, we observe an increase in the Soret band (320 nm) and a new shoulder that appears between 287 and 300 nm and this tendency is amplified for the 1:2 molar ratio. These features are in agreement with the UV visible spectra of CoPcs bearing apical pyridine ligands[7] and according to recent studies, this feature appearing at 288 nm in the Soret band corresponds to metal to ligand charge transfer (MLCT) transition[8].

Unfortunately, the Soret band appears in the same region as the NPLs transition making UV-visible only useful for the detection of CoPcs in the composites without any insight about their binding mode. Nevertheless, this preliminary study shows that MP is a convenient ligand in order to take advantage of the apical positions of CoPc molecules in building molecular-based architectures.

III. 2 Composite material made of CoPc and CdSe NPLs by addition of a bridging ligand

III. 2. 1 Synthetic strategy

The target material is schematically depicted on figure 3a. We intended to sandwich a layer of CoPc between individual NPLs. In order to direct this assembly towards longitudinal stacks we decided to use bridging apical ligands able to link the CoPc by a coordination bond and the NPL by a strong link. We therefore chose 4-mercaptopyridine (MP) as the bridging ligand since it can bind to Co(II) ions by a N-Co dative bond and to CdSe through a S-Cd bond. This strategy involves two alternative routes: either preparing first the [CoPc$(MP)_2$] complex and reacting it with NPLs (figure 3b) or on the contrary, functionalizing first the NPLs with MP and then associating these hybrid particles to CoPc (Figure 3c). We tried both strategies but abandoned the first one after several tries. Indeed after reaction of [CoPc$(MP)_2$] on NPLs, the UV-visible spectra does not show any shift of the excitonic transition. We suspect too much steric hindrance to allow an efficient substitution of surface oleates by the bulky Co(II) complex. We therefore chose the second route because on the contrary, thiolate ligands of small MP ligands strongly bind to CdSe nanoparticles in a first step thanks to the excess of MP that one could use in the reaction. Then, particles bearing an excess of pyridine groups displace the coordination equilibrium towards the formation of the apically substituted CoPcs directly at the surface of NPLs.

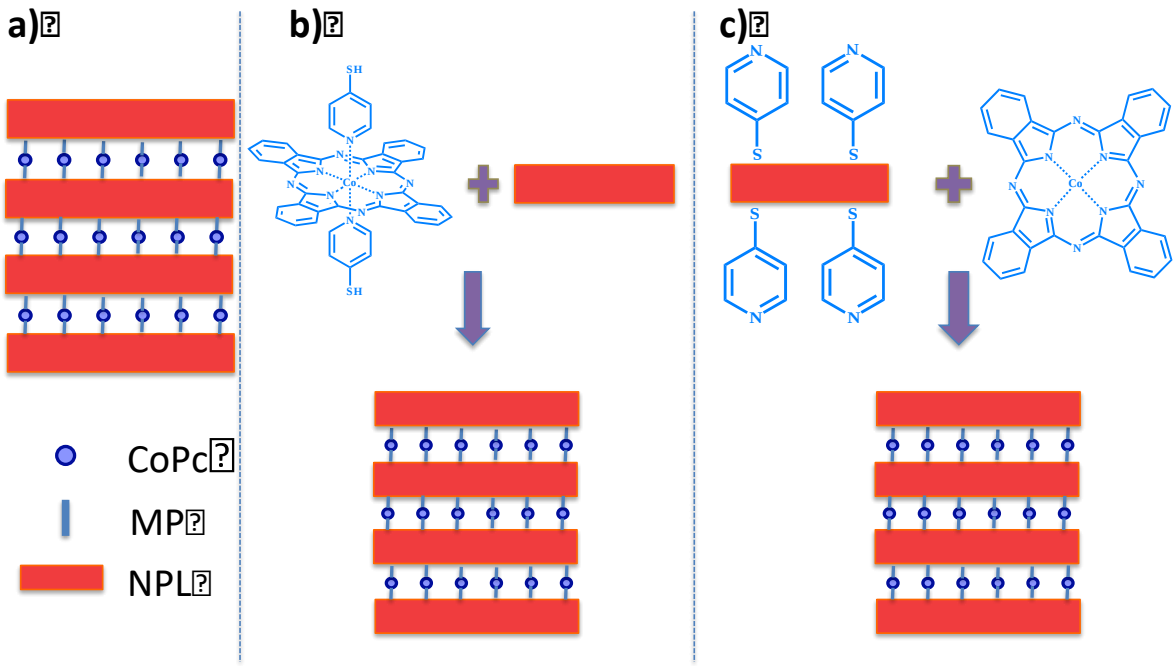

Figure 3: target material (a) and synthetic strategies to get it: reacting [CoPc(MP)$_2$] with NPLs (b) or reacting CoPc with NPLs@MP (c)

III. 2. 2 Results

At first, a UV-visible spectrum (figure 4) has been recorded after having thoroughly eliminated the excess of CoPc by cycles of centrifugation and dispersion and compared to spectra recorded at previous steps of the synthesis.

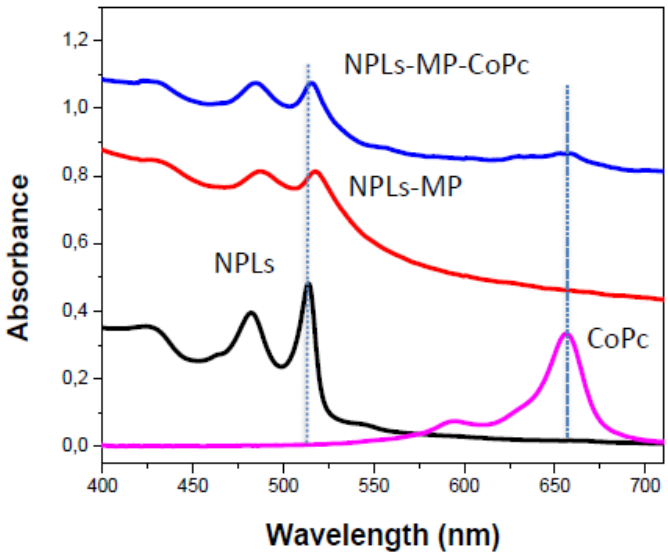

Figure 4. UV-visible spectra of initial NPLs (black) in $CHCl_3$, after reaction with MP (red) in EtOH, after reaction with CoPc (blue) and pure CoPc in THF (magenta)

This spectrum gives the initial signal of NPLs before functionalizing by MP (black). The excitonic hh transition initially lies at 513 nm. Upon functionalization with MP (red), this signal redshifts to 518 nm revealing the exchange of native carboxylate by MP at the surface of the NPLs. After reaction with CoPc (blue), this excitonic transition shifts back to 516 nm indicating that MP is still bound to the surface of NPLs but that the electronic environment of the NPLs is modified towards a better confinement. The modification of the environment of the particles can be related to the presence of the CoPc molecules as indicated by the appearance of the Q-band of the CoPcs at 657 nm. Thus, UV-visible spectroscopy shows that a hybrid material has been obtained by associating CoPc, MP and NPLs.

In addition to UV-visible spectroscopy, Raman spectroscopy is often considered as a valuable tool for the characterization of metallophthalocyanine complexes in the literature. Indeed, their Raman spectra are generally sharp and intense, can be resonance enhanced and they are now quite easy to interpret, in particular with the help of DFT calculations.[9] This

technique may be thus suitable for their routine characterization in many matrices. However, some fluorescence problems may occur with such molecules, but the use of high excitation wavelengths (in the present study at 785 nm) generally prevents these phenomena.

The solid-state Raman spectrum (excitation wavelength at 785 nm) is displayed figure 5 in the range 450-1800 cm^{-1} and showed the characteristic bands of the organic ligand. These bands are attributed to the combination and/or overtone of vibrations within the approximately D_{4h} symmetry core of the ligand. Interestingly, one band (in the range 1490 to 1550 cm^{-1}) has been identified as characteristic of the presence of the metal ion.[10] Fortunately, this is generally the most intense band of the spectrum and depending on the size of the metal incorporated, was found to shift up to 60 cm^{-1}. In the case of Co(II) ions, this band is expected at 1535 cm^{-1} and satisfactorily correlates with the experimental position (1530 cm^{-1}).

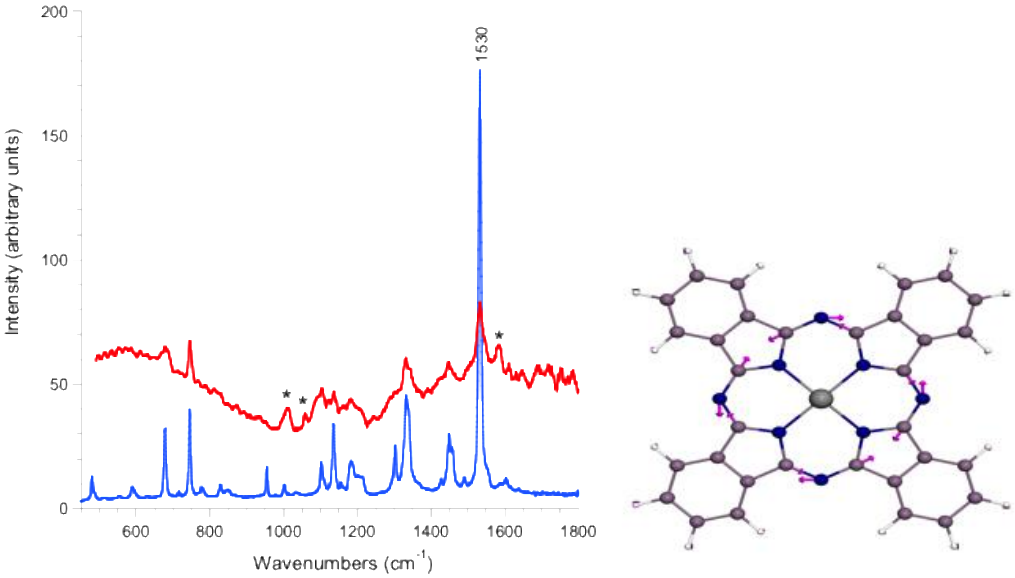

Figure 5: left: solid-state Raman spectrum of CoPc (blue) and NPLs@MP@CoPc (red); right : B_1 vibration mode corresponding to the band at 1530 cm^{-1}

The Raman spectrum of the material obtained after reaction of CoPc with NPLs@MP was then recorded on a solid-state sample obtained after centrifugation of the colloidal suspension (figure 5). The comparison of this spectrum with that of the mass sample of [CoPc] complex is instructive. Indeed, most of the bands observed on the spectrum of NPLs@MP@CoPc may be superimposed with that of the complex alone, confirming thus the presence, but also the integrity of the complex at the surface of the NPs after the deposition

step. In addition, a few peaks were however observed (marked with an asterisk in figure 5) which might hardly be attributed to the complex.

In order to check if these bands were due to the presence of the mercaptopyridine ligands at the surface of the NPs, solid samples of [CoPc] with 1 and 2 equivalents of mercaptopyridine were prepared in parallel. Whatever the amount of mercaptopyridine added, the spectra are identical and it was not possible to characterize the presence of mercaptopyridine in the samples, the band of the phthalocyanine ligands being very intense. Such intensity corresponds to the resonance or pre-resonance enhancement effect (generally in solid-state) due to interactions with either one or both of the electronic absorption bands of the CoPc (Q and B- band).

In order to get more information about the structure of the hybrid material, TEM images were recorded (figure 6). The images disappointingly reveal short stacks of NPLs of about 30 nm and the presence of some still un-stacked NPLs. Interestingly, the spacing between the nanoparticles is of the order of 2 nm, which is very short, and in accordance (although slightly longer) with the size of [CoPc(MP)$_2$] of 1.5 nm (Avogadro simulation). Despite the shortness of the stacks we can thus conclude that a composite material has been prepared, in which MP links CoPc to NPLs.

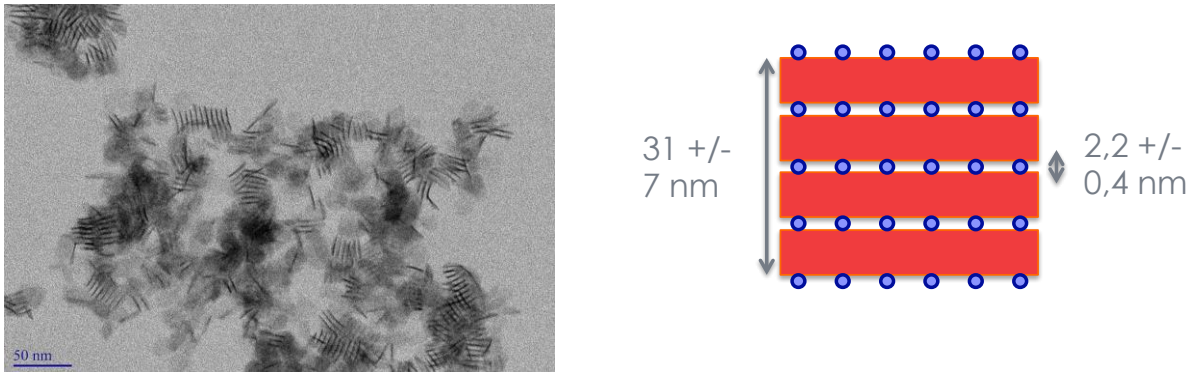

Figure 6: Left: TEM image of the composite material made of CoPc, NPLs ans MP and right: schematic interpretation

The photoluminescence of the NPLs was recorded after each step of the synthesis of the composite (figure 7) at room temperature and in liquid nitrogen. The initial photoluminescence appears as a sharp signal at 513 nm (figure 7a). After functionalization by MP, the luminescence spectra show a very broad and intense signal covering almost all the

visible range and characteristic of exciton trap states that can sometimes appear after exchange of the native carboxylates by other ligands at the surface of CdSe nanocrystals (figure 7a). One can notice a shoulder at 519 nm on this broad signal, attributed to the excitonic relaxation of the NPLs that is 6 nm red-shifted with respect to the initial excitonic signal.

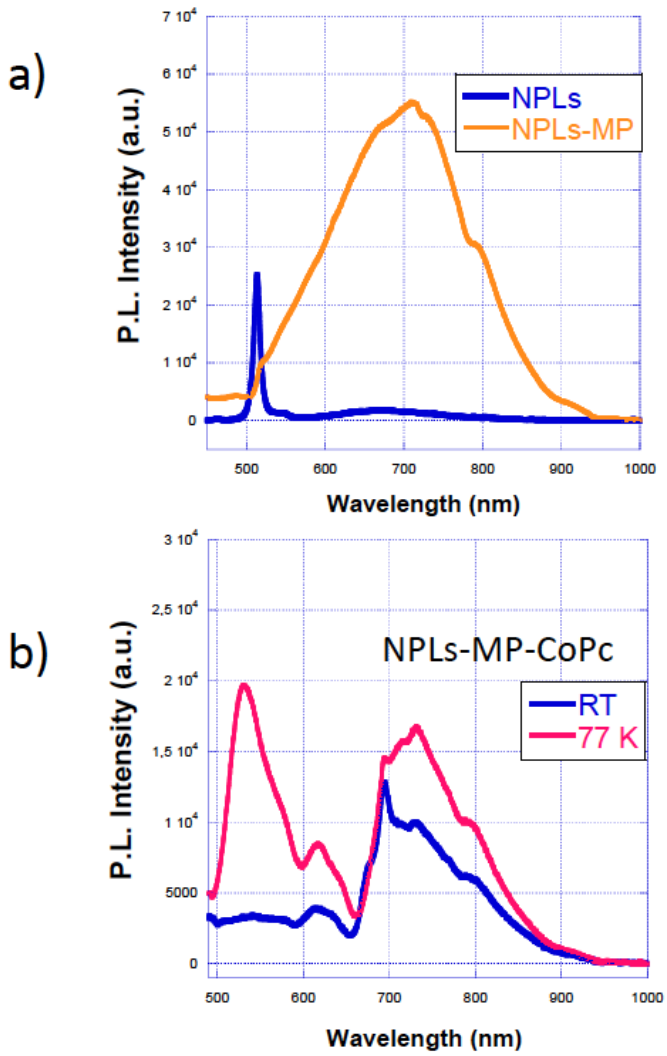

Figure 7: photoluminescence spectra of initial NPLs (a, blue), NPLs@MP (a, orange), NPLs@MP@CoPC at room temperature (b, blue) and NPLs@MP@CoPc at 77K (b, pink)

After reaction with CoPc, the spectra become more complex (figure 7b) with a series of transitions that are modified upon cooling to 77K. The complexity of the photoluminescence is understandable with regards to the TEM analysis. Indeed, even if stacks are in majority, a mixture of different objects is present in solution: maybe some single

unreacted nanoplatelets (minority), single nanoplatelets bearing some CoPcs attached at their surface, stacks of lengths varying between about 20 and 40 nm and even the presence of dimers of NPLs linked by MPs without CoPcs cannot be excluded. Between all these nano-objects, reabsorption of emitted light and energy transfers can easily occur giving rise to a series of signals. Changing the temperature modifies the kinetic of these exchanges allowing the exaltation of some signals and the extinction of others.

III. 2. 3 Discussion

The spacing between the platelets (TEM), associated to the UV-visible and Raman spectroscopies results, confirms the validity of the grafting strategy involving the formation of a lamellar composite material. Nevertheless, the size of the composite particles is not controlled leading to a mixture that makes the interpretation of photoluminescence measurements almost impossible. In order to improve this synthesis it is important to identify all the parameters that drive the assembly and to propose a hypothesis about the mechanism of formation of the composite.

At first, NPLs@MP are not dispersed in THF. Upon mixing with CoPc dissolved in THF, the mixture suspension becomes limpid indicating the dispersion of the NPLs by coordination with CoPc. This suggests that initial oleates at the surface of the NPLs have been removed upon functionalization with MP. This is possible thanks to the treatment of the initial NPLs with $Cd(OAc)_2$ before reaction with MP (**section II. 5. 1**)

Assembly may then arise in a second step. Indeed the inter-particle distance within the stacks observed by TEM cannot be attributed to initial aggregated NPLs@MP that would present an even shorter inter-particle distance. Three types of interactions could thus only drive the stacking: π–π interactions between CoPc complexes and/or depletion interactions (see chapter 2) and/or H aggregates with Co-Co interactions. Coordination interactions would then be excluded since all MP moieties of each NPL are covered in a first step by CoPc molecules. The inter-particle space would then be occupied by a double layer of $[CoPc(MP)_1THF]$ rather than a single layer of $[CoPc(MP)_2]$, in agreement with the slightly increased interparticle distance with regard to the expected size of a single layer. A simulation gives a distance of 2.1 nm for a double layer of $[CoPc(MP)_1THF]$. Unfortunately, this hypothesis cannot be verified since we have shown that the apical coordination of MP on CoPc is detectable only on the Soret band, which is hidden by the absorption of NPLs.

Among the three types of interactions between NPLs proposed above to explain the stacking, π–π interactions between CoPc complexes can be excluded because these molecules are soluble in THF thanks to its coordination to Co ions that separates complexes from each other. H aggregates cannot form since THF is used as the solvent. In the end, only depletion interactions can explain the formation of stacks. But then, why would we get short stacks rather than longer ones like Abécassis?[11] Our hypothesis is that the stacking is an equilibrium leading to an average size of stacks of about 30 nm. In the case of Abécassis this equilibrium is certainly displaced towards longer assemblies, because in his case Van der Waals interactions between alkyl chains can stabilize the stacks.

III. 3 Composite material made of CoPc and CdSe NPLs by weak interactions

III. 3. 1 Synthetic strategy

Recently, Dubertret and co-workers demonstrated that addition of ethanol (polar solvent) into the solution of the NPLs dissolved in a non-polar solvent stacks the NPLs in long anisotropic columns (see chapter I). So we decided to adopt a similar method but, instead of using ethanol as antisolvent for the oleate-capped NPLs we used THF, an aprotic and moderately polar solvent that is known to induce aggregation due to interparticle forces.

Another advantage of the THF solvent is the almost no quenching effect on the CdSe NPLs emission, whereas the ethanol solvent was found to have a quenching effect on the nanoparticles. The addition of ethanol to the NPLs solution may induce the expulsion of the native surface ligands, which may lead to an increasing number of nonemissive NPLs. In addition, CoPc molecule is hardly soluble in many conventional solvents but dissolves quite well in THF.

The first synthetic strategy described in this chapter leads to uncontrolled size of composite particles. In order to simplify the parameters we decided not to try driving the assembly by coordination chemistry but by letting supramolecular interactions triggering it. We thus simply decided to mix initial oleate-covered NPLs with CoPc. In this case, CoPcs are not covered with MP. THF, in which CoPcs are dissolved, cannot disperse NPLs anymore. The only driving forces for assembly are thus depletion interactions and more importantly anti-solvent interactions. We expect then the trapping of CoPcs in-between NPLs; the stability

of the assembly being then ensured by CH-π interactions between alkyl chains of oleates and Pc ligands. CH-π interactions are amongst the weakest. Nevertheless, we believe that weak interactions, when added to each other, can lead to complex supramolecular architectures. This can lead in the end to strong assemblies.

III. 3. 2 Results and discussion

Once more, after thorough removing of the excess CoPc, UV-visible spectra are recorded (figure 8), revealing the presence of the CoPc complexes in the final material since both the NPLs excitonic transitions and the Q band of CoPc are observed.

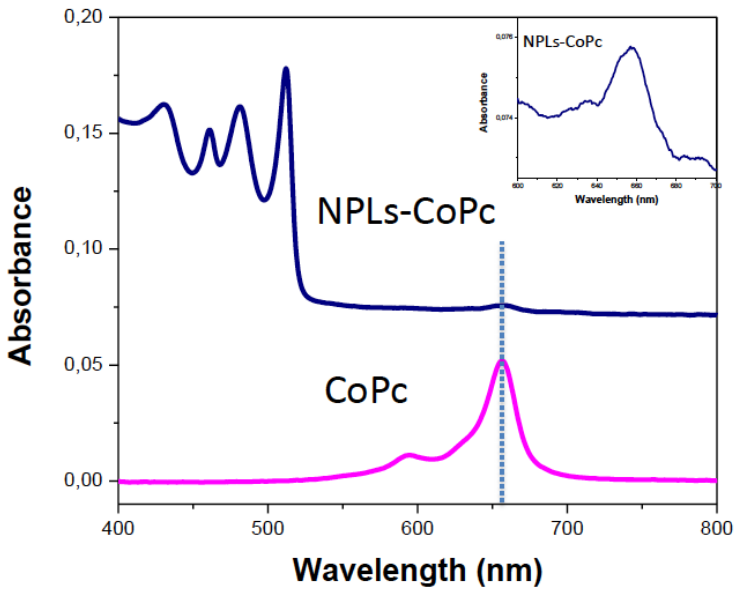

Figure 8. UV-visible spectra of the initial CoPc in THF (pink) and the NPLs@CoPc (navy) in THF. Insertion of the magnification of NPLs –CoPc magnification

TEM images have also been recorded (figure 9). In this case one can observe very long stacks of about a micron bearing an inter-particle distance of 4.5 nm and scarce single NPLs.

In this case, the lack of isolated particles and the length of the stacks indicates that assembly was driven by an efficient force and the length of the stacks as well as the inter-particle distance is coherent with the ones reported by Guzelturk and Demir[12]. This confirms that anti-solvent forces drive the assembly mechanism.

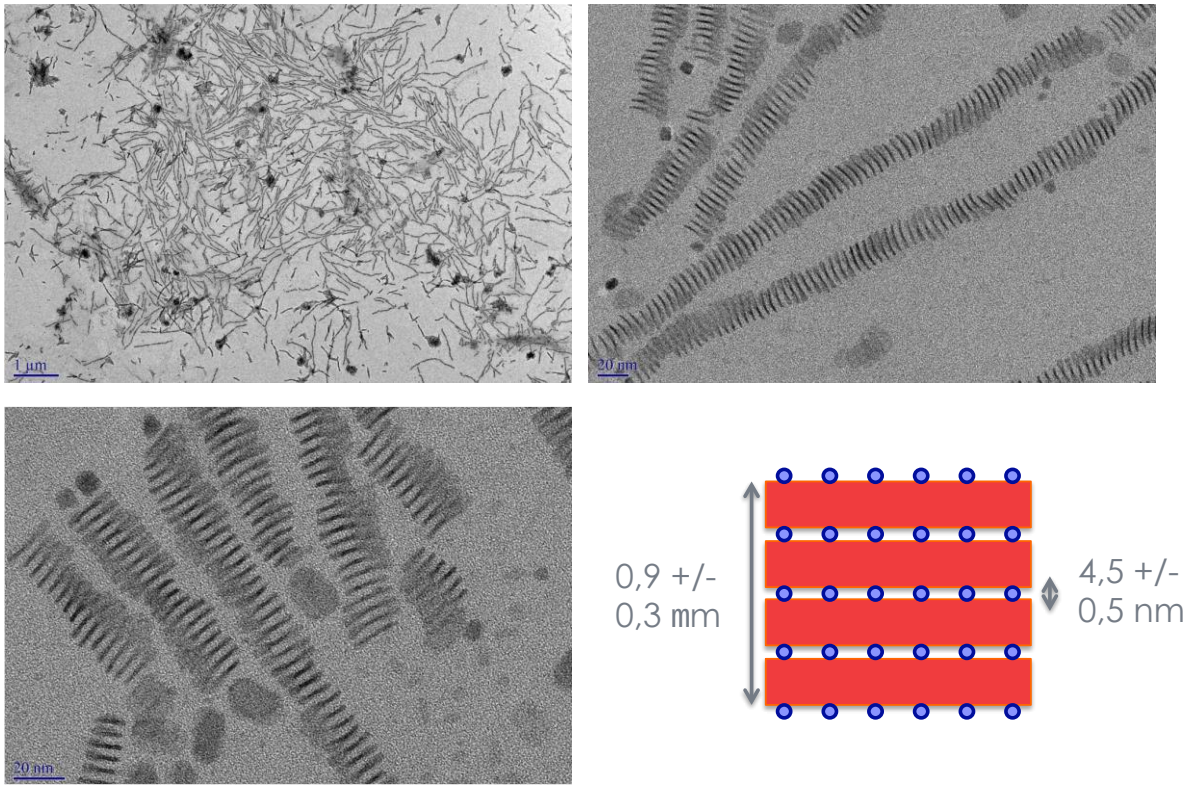

Figure 9: TEM images of the composites obtained by mixing oleate-capped NPLs with CoPc. Scales bars are 1mm (top left) and 20 nm (top right and bottom left). A scheme is given to help the reading of the images.

Photoluminescence spectra have been recorded on these composites. We observed that when the NPLs solution was mixed with the CoPc solution in THF, the emission spectrum at room temperature of stacked NPLs induced by the THF was similar to unstacked NPLs with a single sharp signal at 512 nm. However, we noticed that the excitonic emission of stacked NPLs shifts to 494 nm as the temperature is decreased to 77 K (figure 10). This phenomenon has been reported in semiconductors as CdSe QDs and recently in unstacked CdSe NPLs[13]. Varshni model suggests that the band gap increases as temperature decreases in semiconductors because of electron-phonon interaction, although there are other models that consider the contribution of the lattice expansion to determine the energy gap shift as a function of the temperature.[14]

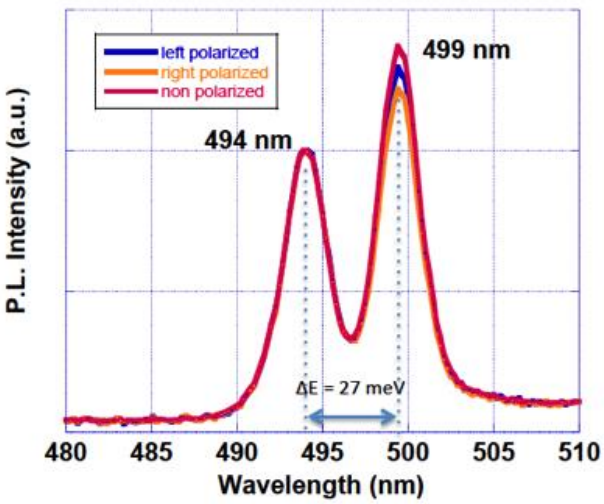

Figure 10: normalized photoluminescence spectra of the composite material made of CoPc and oleate-capped CdSe NPLs recorded at 77K

More interestingly, at 77 K, the spectrum of the stacked nanoplatelets displayed a second emission signal at 499 nm. The energy difference between the excitonic emission and the second low energy emission is around 27 meV. This value is in agreement with the observations of Tessier and co-workers on NPLs assemblies in a mixture of hexane and ethanol. The authors related the high-energy emission (494 nm) to the band edge transition and the low energy emission (499 nm) to a phonon replica (see chapter I).

A surprising phenomenon arises when the same experiment is done under a magnetic field. Under about 1T, the phonon line is circularly polarized (figure 11) although it was not in the absence of magnetic field.

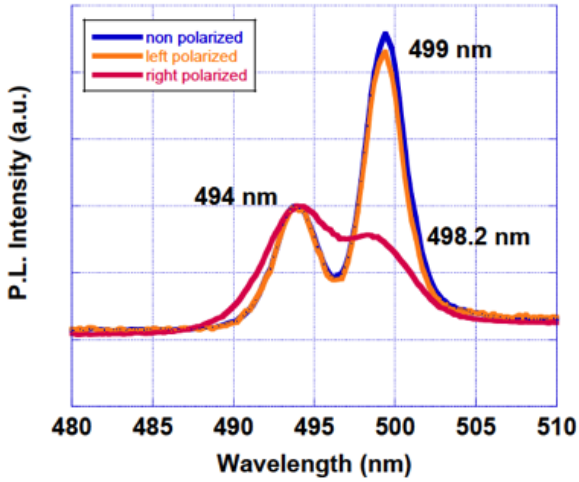

Figure 11: normalized photoluminescence spectra of the composite material made of CoPc and oleate-capped CdSe NPLs recorded at 77K

Circularly polarized light is the manifestation of a symmetry breaking. This symmetry breaking can be a spatial symmetry breaking *i.e.* in a media that lack mirror symmetry (a chiral media) and the phenomenon is known as natural optical activity (NOA). In our system, neither NPLs nor CoPc are chiral, therefore NOA is unlikely. Moreover, NOA would have been observable in the absence of applied magnetic field. On the contrary, magnetic optical activity (MOA) arises under a magnetic field and represents a difference in absorption and refraction between left and right circularly polarized light. An application of MOA is magnetic circular dichroism (MCD) spectroscopy laying on the fact that a paramagnet under a magnetic field absorbs differently right and left circularly polarized light because of spin-orbit (so) coupling in the excited state. In our system we therefore suspect Co(II), whom is submitted to such coupling, to be responsible for the dichroic signal that we observed.

We therefore sought to understand how the phonon line (intrinsic to NPLs) could be influenced by the spin alignement of CoPcs under magnetic field. The only semiconducting material submitted to MOA is GaAs because of strong so coupling. From initial works of Khaetskii and Nazarov,[15,16] on GaAs, Loss and co-workers[17] derived an effective Hamiltonian, which couples the electron spin to phonons. Their study reveals that the strain field produced by phonons couples to the electron spin via the so coupling.

In our system we propose that the phonon couples to localized Co(II) spins. In other words, under a magnetic field, the spins of Co(II) ions align in the direction of the field and the resulting magnetization is then felt by the phonon. As a consequence the phonon preferably absorbs light in a given polarization. That would explain the polarization of the phonon line emission observed on figure 11.

III. 4 Conclusion and perspectives

About the first strategy involving MP, we can conclude that the functionalization of the CdSe nanoplatelets with MP ligands leads to a red-shift in UV-Vis spectroscopy denoting an effective exchange ligand of native carboxylate by the thiol anchoring ligands. In addition, the interaction between NPLs@MP hybrids and CoPc molecules displayed then a blue-shift, revealing modifications of the electronic environment of the NPLs induced by the CoPc molecules. The presence of these CoPc molecules is also confirmed by Raman spectroscopy that reveals the formation of the NPLs@MP@CoPc hybrid material.

Contrary to what we expected, the formation of the NPLs assembly (analyzed by TEM images) might be triggered by depletion interactions rather than by the formation of the bridging coordination complex [CoPc$(MP)_2$] linking two nanoplatelets. Indeed, the interparticle distance suggests a possible interaction of the NPLs with a double layer of [CoPc(MP)THF]. We believe that the NPLs assembly driven by the coordination of [CoPc$(MP)_2$] could be achieved by adding dropwise the NPLs@MP@CoPc hybrids that we obtained to NPLs@MP in order to displace the coordination equilibria towards the formation of the target composite.

Another alternative is to build up the composite layer-by-layer from a planar substrate (Fig. 12). This method was already implemented by initially grafting the NPLs to a glass substrate previously functionalized by (3-mercaptopropyl)trimethoxysilane. This first layer reacts then sequentially with MP, CoPc, MP and NPLs to stepwise form stacked NPLs-CoPc-NPLs sandwiches. Such a method seems promising since it paves the way to structures of greater complexity by the use of different metallophthalocyanines or complexes and because it allows getting rid of most of solubility issues.

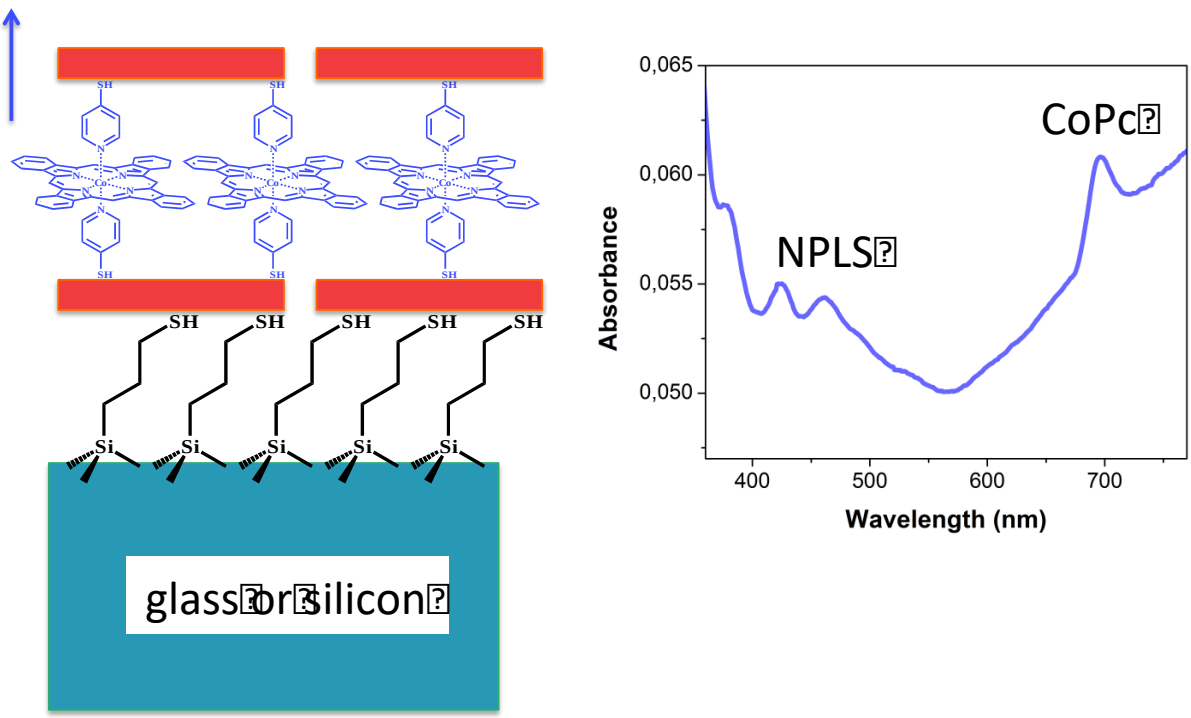

Figure 12. Schematic representation of the layer-by-layer deposition strategy (left) and preliminary result: UV-visible spectrum of a glass slide covered with the first layer of NPLs and of CoPc molecules on which one can identify both the Q-band of CoPc and the excitonic transitions of NPLs.

From the results obtained by strategy 2, we conclude that the mixture of CoPc and NPLs leads to the assembly of the NPLs, which is triggered by depletion interactions and anti-solvent effects. Such NPLs assembly apparently traps CoPc species within the nanoparticles by CH-π interactions between the alkyl chains of the oleates and the phthalocyanines. The presence of the CoPc was confirmed by UV-Vis spectroscopy.

Moreover, by means of photoluminescence techniques, we discovered on such a composite material at low temperature and under a magnetic field an unexpected phenomenon that can be explained by collective properties. This shows that our system allows the amplification and expression of molecular properties while the molecules are present in small quantities.

III. 5 Experimental section

Synthesis of [CoPc(MP)$_x$] x= 1, 2

The complexes solutions were prepared with 3 ml of CoPc (2.19 x 10^{-4} mol.L^{-1}) and 24 µL of MP (0.027M) solution in THF, at a molar ratio CoPc:MP of 1:1. Also, 3 ml of CoPc solution and 48 µL of MP in THF were prepared, at a molar ratio CoPc:MP of 1:2. Both reactions were stirred during 1 h, in the dark.

Synthesis of NPLs@MP@CoPc (section III.2)

- Preparation of NPLs

The CdSe nanoplatelets were synthesized (**annex A**) and purified with EtOH. After centrifugation, the NPls were treated with $Cd(OAc)_2$ according to the **section II.4.5.1** Then, the NPLs were precipitated in EtOH and redispersed in $CHCl_3$. The concentration of the NPLs was prepared at 3.06 x 10^{-8} mol.L^{-1}.

- Ligand exchange and CoPc reaction

300 µL of Mercaptopyridine (MP) solution (0.027 mol.L^{-1}) were added to 2 ml of CdSe NPLs solution in the dark and we let the reaction run for 20-25 min. After the reaction, the NPLs changed from yellow color to orange color. The precipitate was centrifugated and redispersed in 2 ml of CoPc complex solution (2.19 x 10^{-4} mol.L^{-1}) in THF previously micro-filtered by sonication and stirred during 1 h.

The microstructure of the NPLs@CoPc, was examined with transmission electron microscope (TEM). For the TEM study a drop of NPLs@MP@CoPc were immediately put onto TEM the copper grids and let it dry over night.

The NPLs@MP@CoPc were collected by centrifugation at 12000 rpm and redispersed in THF to remove the excess of CoPc. The washing procedure was repeated one more time. Then, the NPLs@MP@CoPc were redispersed in 1 ml of THF.

All the optical measurements were performed by JASCO V-670, UV-Vis spectrophotometer used for the absorption spectra and by Ocean Optics Miniature fluorimeter for the photoluminescence spectra.

Synthesis of NPLs@CoPc (section III.3)

The CdSe nanoplatelets nanoplatelets were synthesized (**annex A**) and purified with EtOH. After centrifugation the NPLs were redispersed in $CHCl_3$ and the concentration was set up to 3.06 x 10^{-8} mol.L^{-1}. In 1 mL of NPLs were added 2 ml of CoPc complex solution (2.19 x 10^{-4} mol.L^{-1}) in THF previously micro-filtered and stirred during 20 min.

The microstructure of the NPLs@CoPc, was examined with transmission electron microscope (TEM). For the TEM study a drop of NPLs@CoPc solution was put onto TEM copper grid and allowed to dry overnight.

For UV visible spectra, the NPLs@CoPc were collected by centrifugation at 12000 rpm during 5 min and redispersed in THF through sonication to remove the excess of CoPc molecule. Then, the precipitated was redispersed again in THF and the washing procedure was repeated one more time. Finally, the NPLs@CoPc were redispersed in 1 ml of $CHCl_3$ and THF (ratio 1:2) solution.

III. 6 References

1 S. Arslan, Phthalocyanines: Structure, Synthesis, Purification and Applications.

2 C. G. Claessens, U. Hahn and T. Torres, Phthalocyanines: From outstanding electronic properties to emerging applications, *Chem. Rec.*, 2008, **8**, 75–97.

3 H. Isago, *Optical Spectra of Phthalocyanines and Related Compounds*, Springer Japan, Tokyo, 2015.

4 G. Löbbert, in *Ullmann's Encyclopedia of Industrial Chemistry*, ed. Wiley-VCH Verlag GmbH & Co. KGaA, Wiley-VCH Verlag GmbH & Co. KGaA, Weinheim, Germany, 2000.

5 F. Ghani, J. Kristen and H. Riegler, Solubility Properties of Unsubstituted Metal Phthalocyanines in Different Types of Solvents, *J. Chem. Eng. Data*, 2012, **57**, 439–449.

6 T. Nyokong, Equilibrium and kinetic studies of the reaction between pyridine and cobalt(II) phthalocyanine in DMSO, *Polyhedron*, 1995, **14**, 2325 – 2329.

7 I. Ponce, J. F. Silva, R. Oñate, S. Miranda-Rojas, A. Muñoz-Castro, R. Arratia-Pérez, F. Mendizabal and J. H. Zagal, Theoretical and Experimental Study of Bonding and Optical Properties of Self-Assembly Metallophthalocyanines Complexes on a Gold Surface. A Survey of the Substrate–Surface Interaction., *J. Phys. Chem. C*, 2011, **115**, 23512–23518.

8 M.-S. Liao and S. Scheiner, Electronic structure and bonding in metal phthalocyanines, Metal=Fe, Co, Ni, Cu, Zn, Mg, *J. Chem. Phys.*, 2001, **114**, 9780–9791.

9 D. R. Tackley, G. Dent and W. Ewen Smith, Phthalocyanines: structure and vibrations, *Phys. Chem. Chem. Phys.*, 2001, **3**, 1419–1426.

10 G. Dent and F. Farrell, NIR FT Raman examination of phthalocyanines at 1064 nm, *Spectrochim. Acta. A. Mol. Biomol. Spectrosc.*, 1997, **53**, 21 – 23.

11 S. Jana, P. Davidson and B. Abécassis, CdSe Nanoplatelets: Living Polymers, *Angew. Chem. Int. Ed.*, 2016, **55**, 9371–9374.

12 B. Guzelturk, O. Erdem, M. Olutas, Y. Kelestemur and H. V. Demir, Stacking in Colloidal Nanoplatelets: Tuning Excitonic Properties, *ACS Nano*, 2014, **8**, 12524–12533.

13 M. D. Tessier, C. Javaux, I. Maksimovic, V. Loriette and B. Dubertret, Spectroscopy of Single CdSe Nanoplatelets, *ACS Nano*, 2012, **6**, 6751–6758.

14 Y. P. Varshni, Temperature dependence of the energy gap in semiconductors, *Physica*, 1967, **34**, 149 – 154.

15 A. V. Khaetskii and Y. V. Nazarov, Spin relaxation in semiconductor quantum dots, *Phys Rev B*, 2000, **61**, 12639–12642.

16 A. V. Khaetskii and Y. V. Nazarov, Spin-flip transitions between Zeeman sublevels in semiconductor quantum dots, *Phys Rev B*, 2001, **64**, 125316.

17 V. N. Golovach, A. Khaetskii and D. Loss, Phonon-Induced Decay of the Electron Spin in Quantum Dots, *Phys Rev Lett*, 2004, **93**, 016601.

Conclusion

Conclusion

During this Ph.D. we intended the design and synthesis of new nanomaterials based on CdSe NPLs and coordination compounds. At the beginning we sought for synergies between the optical properties of the NPLs and the magnetic properties of the coordination complexes to be grafted onto the particles. This project was therefore very challenging since we had no idea whether such synergies could take place or not. The only clue we had was that in 2015 the optical properties of CdSe NPLs were predicted to be original, although at this time the literature on this subject was scarce and sometimes contradictory. At first, a clear and reproducible synthetic method for the preparation of CdSe NPLs has been established during this Ph.D. In particular all experimental details and conditions had to be more precisely settled than it was in the literature. The second challenge was to master the purification of the NPLs and at last, to understand the way the environment of the NPLs could chemically be modified to produce hybrids.

Then, we had to define at which scale we could process the hybrids: on individual particles or in a composite made of several particles associated to complexes? It appeared that the colloidal stabilization of hybrid individual NPLs was a difficult task or even sometimes impossible. However this approach should converge in the future since the groups working on the chemistry of CdSe NPLs only begin to understand the chemical properties of their surfaces. Nevertheless, the work done on the azobenzenes-driven assembly of the NPLs opened up a perspective. Indeed, the understanding of the parameters controlling the stacking of these particles gave us the idea to associate Co(II) phthalocyanines to the NPLs in a layered composite.

Such an approach based on the association of NPLs mediated by metallophthalocyanines lead us to discover collective properties able to reveal an interesting magnetic optical activity. We have therefore shown for the first time in the group that a synergy between paramagnetism and optical properties can arise in such a system. This result opens up perspectives since one can imagine that the phonon line is sensitive to perturbations and could therefore reveal other properties.

From a personal point of view, working with these nanoparticles with such a high level of complexity, opened up another world of Chemistry, unknown to me in my previous

experience; another way to think, to work and to understand such fascinating nanosystems. More importantly, gathering all these experiences to build something interesting and unprecedented, represents to me, why not, a possibility to unravel a little more the unknown and intricate behaviour of nature.

Annexes

Annex A

Synthesis of Nanoplatelets

80 mg of cadmium myristate are dispersed in 15 ml of octadecene (ODE) by sonication during 20 to 30 min and 12 mg of selenium powder are added to the suspension in a three-neck flask and sonication is maintained for 15 min.

The mixture is degassed under vacuum and stirred at 90°C for 1 h. After that, the mixture is heated up to 250°C. At ~135 °C the reaction is placed under argon atmosphere. At ~195°C, when the solution becomes yellow-orange, 82 mg of cadmium acetate $Cd(OAc)_2$ are added. Immediately the solution is degassed several times. The reaction is kept at 250°C for 3 min, and then at 260°C for 3 min and the mixture is let to cool down to 245-250°C over 40 min under argon atmosphere. The reaction was allowed to cool down to room temperature still under argon atmosphere.

Annex B

1) CdSe NPLs functionalization with complex [Mn(TPA)S_2]

a) Strategy 1

Synthesis of [Mn(TPA)(NO_3)$_2$]

2,6 mg of $Mn(NO_3)_2 \cdot 4H_2O$ (0,0145 mmol) were dissolved in 1 ml of formamide (CH_3NO, FA) and 20 mg of triphenylamine (TPA) (0,082 mmol) were dissolved in 2 ml of formamide. The first solution was added to the last solution and the reaction was let out stirred during 30 min.

Synthesis of NPLs@S

On the other hand, 20 mg of Na_2S (0,256 mmol) was dissolved in 2 ml of formamide. This solution was added to 1 ml of NPLs solution (previously purified) in toluene and let out stirring for 1 h. The reaction was stopped after seeing the phase transfer of CdSe NPLs from toluene to the formamide phase. The phase transfer is completed when the color of toluene is colorless. The FA is separated out by washing 3 times with toluene to remove the excess of NPLS that were not grafted and with CH_3CN to precipitate. After that, the NPLs@S were redispersed in 1 ml of FA.

Synthesis of NPLs@S@Mn@TPA

Finally, the NPLs@S solution was added in drops into the [Mn(TPA)(NO_3)$_2$] complex solution. The reaction mixture was let out during 3 days. After the time reaction, the NPLs@S@Mn@TPA solution was not longer fluorescence.

b) Strategy 2

Synthesis of [Mn(TPA)(NO_3)$_2$]

The synthesis was carried out similarly as the previously mentioned with Na_2S with the only difference that they were dissolved in MeOH.

Synthesis of NPLs@S

43 µl of $(NH_4)_2S$ was added in 2 ml of H_2O and drops-wise of this solution were added to 1 ml of the NPLs solution. The color changes as the solution is added to the NPLs. The phase transfer of the CdSe NPLs from $CHCl_3$ to H_2O phase is observed after less than 10 min. The

polar phase is separated out by washing 3 times with $CHCl_3$. The solution was then precipitated out with acetone, and redispersed in 2 ml of MeOH.

Synthesis of NPLs@S@Mn@TPA

The NPLs@S solution was added dropwise to the $Mn(TPA)(NO_3)_2$ and the reaction was kept for 1 day. The precipitate was redisperse in EtOH but the NPLs were dissolved or destroyed.

2) CdSe NPLs functionalization with $[Mn(Ac)_2]$

Synthesis of NPLs@S

3,3 mg of Na_2S (0,042 mmol) were dissolved in 1 ml of formamide. Then, the solution was added to 1 ml of NPLs in $CHCl_3$ and the mixture was stirred during less than 10 min. The non-polar phase was removed from NPLs@S in FA.

Synthesis of NPLs@S@Mn

30 µl of 0,1 M solution of tetramethylammonium chloride was added into the NPLs@S solution in FA. The mixture was stirred for 5 min and then, 60 µl of 0,1 $mol.L^{-1}$ solution of didodecyldimethylammonium bromide (DDAB) in $CHCl_3$ was added. The mixture was let out stirring for 20 min. Then, the $CHCl_3$ phase is separated out and washing 3 times with FA. Finally, 60 µL of 0,1 $mol.L^{-1}$ solution of manganese acetate $Mn(OAc)_2$ in FA is added to the non-polar phase and stirred for 2 min. The nanoplatelets remained in the interfase and were no longer fluorescence.

3) CdSe NPLs functionalization with complex $[Mn(hfac)_2]$

The formation of NPLs@S was similar to the one previously reported (3). Then, 30 µL of 0,1 $mol.L^{-1}$ solution of tetramethylammonium chloride was added to the NPLs@S solution in FA. After 5 min of reaction, 15 µL of 0,1 $mol.L^{-1}$ solution of DDAB in toluene was added and let it stir for 10 min. Then, the non-polar phase was separated out and washing 3 times with FA. Finally, 35 µL of $Mn(hfac)_2$ (hfac = hexafluoacetylacetonate) of 1.28 mM was added to the NPLs@s solution with a reaction time of 24 h.

Nanoplaquettes semi-conductrices hybrides : synthèse et assemblage par l'intermédiaire de molecules

Résumé :

Ce doctorat avait pour objet l'exploration des propriétés chimiques de nanoplaquettes de séléniure de cadmium en les fonctionnalisant par des complexes paramagnétiques de coordination. En effet, l'association des propriétés magnétiques des complexes avec les propriétés optiques très originales de ces objets pourrait conduire à la découverte de nouvelles propriétés magnéto-optiques. Cette thèse, en cohérence avec des résultats récents de la littérature, a confirmé que la forme plaquettaire de ces nano-objets induisait leur empilement lorsqu'ils sont recouverts de ligands appropriés et dispersés dans des solvants adaptés. Cette thèse présente trois chapitres portant sur (*i*) la description des nanoplaquettes de CdSe du point de vue de leur structure et de leurs propriétés, (*ii*) une étude de l'assemblage des plaquettes lorsque celles-ci sont fonctionnalisées par des molécules de type azobenzène isomérisable et (*iii*) l'étude de l'assemblage des nanoplaquettes par l'intermédiaire de phtalocyanines de cobalt(II) conduisant à des matériaux composites. Nous avons montré que la fonctionnalisation des nanoplaquettes par des molécules d'azobenzène permettait leur assemblage hors équilibre c'est à dire sous apport continu d'énergie. Par ailleurs, deux voies d'assemblage des nanoplaquettes avec la phtalocyanine de cobalt ont été explorées. Ces deux voies permettent d'obtenir des composites de structures différentes et dans un cas il a été observé une émission de lumière polarisée circulairement sous champ magnétique. Ce résultat montre l'existence d'une rupture de symétrie dans le composite liée à la présence du complexe de cobalt et donc l'apparition de propriétés magnéto-optiques.

Mots clés : nanocristaux ; nanoplaquettes ; semiconducteurs ; assemblage ; photoluminescence ; hybrides

Hybrid semiconducting nanoplatelets: synthesis and molecule-driven assembly

Abstract:

This Ph.D. aimed at a better understanding of the chemical properties of cadmium selenide nanoplatelets by functionalization by paramagnetic coordination complexes. Indeed, the original optical properties of the platelets associated to the paramagnetism of transition metal complexes could lead to new magneto-optic properties. In agreement with recent literature results, this Ph.D. confirms that the planar morphology of these nano-objets induces their stacking when covered by appropriate ligands and dispersed in appropriate solvents. This thesis presents three chapters about (*i*) the description of the structure and the properties of CdSe nanoplatelets, (*ii*) a study of azobenzene-decorated nanoplatelets and (*iii*) the self-assembly of CdSe nanoplatelets mediated by cobalt(II) phtalocyanines to produce composite materials. This work shows that functionalizing CdSe nanoplatelets with azobenzene moieties allows their out-of-equilibrium assembly. Furthermore, two ways of assembling nanoplatelets with cobalt(II) phtalocyanines have been developed leading to composites bearing different structures. For one of these structures a circularly polarized light is emitted under magnetic field revealing a symmetry braking in the composite thanks to the cobalt complex and thus magneto-optic effects.

Keywords: nanocrystals; nanoplatelets; semiconductor; assembly; photoluminescence; hybrids